Ryu *et al. Chem. Biol. Technol. Agric.* (2024) 11:10
https://doi.org/10.1186/s40538-023-00532-2

Chemical and Biological Technologies in Agriculture

RESEARCH

Open Access

Metabolic modulation of Basil (*Ocimum basilicum* L.): an insight into growth, metabolomics and antioxidant activity under varying temperature and light conditions

Da Hye Ryu[1†], Jwa Yeong Cho[1,2†], Muhammad Hamayun[3], Dong Gyu Lee[1] and Ho-Youn Kim[1,2*]

Abstract

Background Temperature and light are two critical environmental stimuli that greatly impact our agricultural industry. We explored the effects of varying temperature and light conditions on the metabolomics of basil, a plant widely used in cuisine and for medicinal purposes worldwide. Basil plants were subjected to elevated temperatures of 30 °C, 35 °C, and 40 °C, along with two light intensities (D11 and D23).

Results Our results showed that the maximum shoot length (42.98 cm) was achieved at T30 and D23, the maximum leaf area (6.92 cm) at T30/D11, and the highest number of leaves (472) at T40/D11. However, at the higher temperature of T40, the number of leaves increased, but shoot length and leaf size significantly decreased ($p < 0.05$). Maxim shoot biomass (81 gm) and root biomass (91.2 gm) was recorded at T35/D23 treatments. Metabolomic studies of basil revealed that rosmarinic acid (RA), and linalool and eugenol were the major phenolic and volatile organic compounds (VOCs) under different growth conditions. RA levels were higher at 30 °C, correlated with elevated shikimate levels, indicating a carbon supply through the TCA cycle. In contrast, the growth conditions of 35 °C/D11 (μmol/m^2/d) up-regulated the glyoxylate cycle (fumaric acid and malic acid) as part of stomatal closure, preventing ROS accumulation and resulting in increased VOC emission. Exposure to the higher temperature of 40 °C induced higher amino acid accumulation, improving temperature stresstolerance.

Conclusions This study suggests that elevated temperature and light intensity affected the overall health of basil plants by modulating underlying growth mechanisms. Furthermore, elevated temperature plays a vital role in plant defense mechanisms by mediating the production of secondary metabolites associated with plant defense responses.

Keywords Abiotic stress, Elevated temperature, Daily light integral, Defense mechanism, Primary metabolite, Secondary metabolite

[†]Da Hye Ryu, Jwa Yeong Cho contributed equally to this work.

*Correspondence:
Ho-Youn Kim
hykim@kist.re.kr
Full list of author information is available at the end of the article

Graphical Abstract

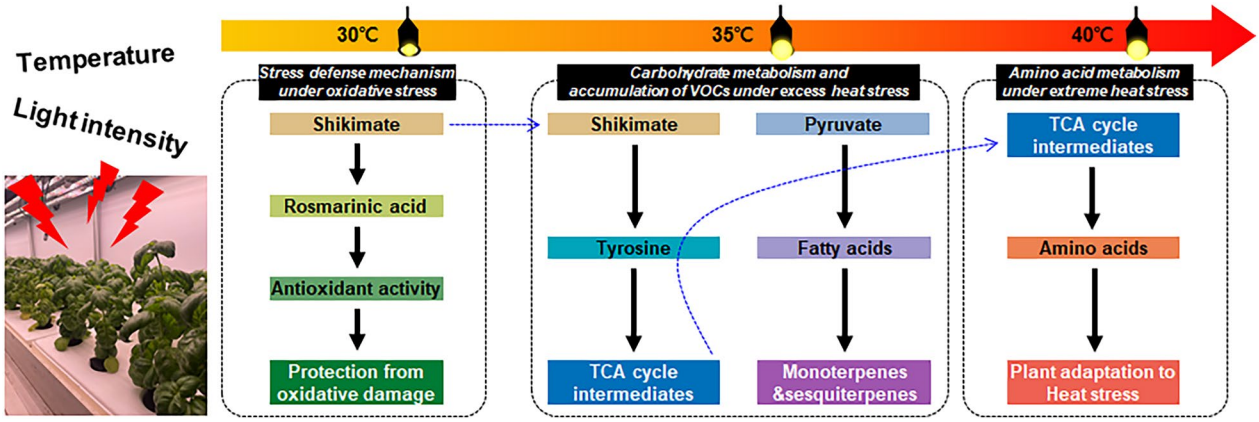

Introduction

Plants are sensitive to environmental stimuli and adaptable to changes in their surroundings [1]. Temperature and light are the most critical environmental cues that influence the growth and development of plants by providing seasonal information [2]. The interrelated and complex effects of temperature and light trigger various plant responses. Light significantly contributes to acclimation responses to both low and high temperatures and can influence the extent of stress damage [3]. Plant photoreceptors, like phytochrome and cryptochrome, crucially recognize the quality, quantity, and direction of light, as well as temperature sensing. They differentially affect phytohormone signaling based on temperature levels [1, 4, 5]. Photoreceptors are responsible for both light quality and high temperatures, showing that photo- and thermo-morphogenesis share a core signaling pathway, indicating their interdependence [6–11]. While normal conditions tend to counteract light signals in stem growth adjustment, a temporary temperature increase supports the light-induced inhibition of hypocotyl growth [12]. Karayekov, Sellaro [12] demonstrated that the high-temperature response in Arabidopsis depends on the presence or absence of light, with a significant effect in response to light but not in the dark. Additionally, various developmental processes, such as seed germination, seedling de-etiolation, vegetative growth, and flowering, are induced by unfavorable conditions [6, 7]. These responses are considered part of the defense mechanism activated by plants to perceive environmental stimuli and minimize damage from challenging conditions [2, 13].

Under unfavourable environmental conditions, such as heat stress, plants experience reduced productivity and shortened life cycles due to diminished photosynthetic efficiency and compromised photochemical reactions [14]. Additionally, secondary metabolite accumulation contributes to environmental adaptation and acts as a defense mechanism against external stimuli [15]. Temperature stress can also lead to the accumulation of reactive oxygen species (ROS) in plant cells, resulting in lipid peroxidation, enzyme inactivation, nucleic acid and protein degradation [16, 17]. To counteract these stresses, plants activate various non-enzymatic antioxidants, such as phenolics, flavonoids, carotenoids, and glucosinolates, serving as a non-enzymatic defense mechanism against both biotic and abiotic stressors [14, 18]. These well-documented secondary metabolites are of high value due to their utility, and efforts have been made to enhance their biosynthesis pathways and content [19]. Rosmarinic acid (RA) found in *Lamiaceae* plants is renowned for its value in plant defense mechanisms and pharmacological activities. RA directly scavenges ROS and indirectly suppresses various disease mechanisms, including cancer, diabetes, aging, cardiovascular disease, and inflammation [20]. Up-regulated genes involved in RA biosynthesis under abiotic stress, such as tyrosine aminotransferase and rosmarinic acid synthase, have been reported [21–24]. In addition to RA, VOCs act as stress response metabolites. In basil, produced VOCs are essential constituents participating in antimicrobial activity [24], antioxidant capacity [25], and anti-fungal ability [26]. These small molecules (less than 300 Da) derive from diverse biosynthetic pathways related to fats, lipids, amino acids, and proteins [27]. They are emitted from the cuticle, stomata, or wounded tissues and serve as physiological defense signals, with biogenic VOCs being emitted more under

stressed conditions [28]. Stress-induced VOC emissions can interact with neighboring plants to signal stress occurrence and affect plant phenotypic responses [29]. When exposed to mild stress, plants perceive it as a signal and activate various defense systems. These defense systems involve the production of antioxidant enzymes and secondary metabolites, playing critical roles in their adaptation and defense against stress [30, 31].

The hypothesis of this study was based on the induction of secondary metabolite biosynthesis at elevated temperatures would differ depending on the quality of light intensity. Previous research by Walters and Currey [32] on basil demonstrated that yield was proportional to temperature up to 30 °C, but a decrease in node appearance rate and fresh weight occurred at 35 °C. However, this finding was based on experiments conducted under specific light intensity conditions, and the effects of the interaction between light intensity and temperature on basil productivity and functionality were not thoroughly explored. To investigate the impact of temperature and light intensity as mild stressors, this study examined various temperature conditions (normal, 30 °C; mild heat, 35 °C; and extreme heat, 40 °C) and daily light integral (DLI; low, 11 μmol/m^2/d; and high, 23 μmol/m^2/d) on basil.

$$\mathrm{DLI} = \frac{\mathrm{PPFD}\left(\mathrm{x}\ \frac{\mu\mathrm{mol}}{\frac{\mathrm{m}^2}{\mathrm{s}}}\right) \times 60\ \frac{\mathrm{min}}{\mathrm{hr}} \times 60\ \frac{\mathrm{sec}}{\mathrm{hr}} \times \mathrm{Photoperiod\ (hr)}}{1,000,000\ \frac{\mu\mathrm{mol}}{\mathrm{mol}}}$$

Material and methods

Plant cultivation

Basil (*Ocimum basilicum* L.) seeds were obtained from World Seed Company in Gwangju, South Korea. Seeds were sown individually in 200-cell plug trays filled with rock wool plugs manufactured by Grodan Rockwool BV in the Netherlands. To maintain the seed moisture contents, the rock wool plugs were watered for the initial 14 days, and then the electric conductivity (EC) was gradually increased. The nutrient solution used consisted of 3.16 mM NO^{3-}, 0.77 mM NH_4, 0.32 mM PO^{4-}, 5.99 mM K, 4.00 mM Ca, 2.00 mM Mg, and 0.67 mM SO^{4-}. Before transplanting, the EC levels were incrementally adjusted, maintaining them at 0.5 dS/m from 13 to 19 days after sowing (DAS) and at 0.75 dS/m from 20 to 27 DAS. During the germination period, the plants were exposed to a light intensity of 200 ± 11 μmol/m^2/s from fluorescent lamps (Philips Korea, Seoul, South Korea) on a 14:10 h light/dark cycle at temperatures of 18/25 °C (day/night) and within a relative humidity range of 50–80%.

Plant growth condition

Germinated basil seedlings with 6–7 leaves were transplanted into a small-sized vertical farm. The farm was equipped with real-time environmental monitoring using a CO_2 sensor module (KCD-HP100, Korea Digital Co., LTD, Seoul, South Korea), a temperature and humidity sensor module (KSH-7310, Korea Digital Co., LTD, Seoul, South Korea), and a cooling and heating system to regulate the desired temperature conditions. The lighting conditions were set to a 14:10 h light/dark cycle, and the light intensity was controlled by LEDs consisting of a mixture of 11 white LEDs, 4 blue LEDs (454 nm), and 7 red LEDs (658 nm) (KLB-40-2C; KAST Engineering, Gumi, South Korea). For specific planting densities and cultivation system configurations, please refer to Fig. 1. To investigate the optimal growth conditions for basil, different daily light integral (DLI) and temperatures regimen were applied as follows. DLI was calculated using the following formula:

Basils were cultivated under diverse conditions by varying DLI and temperatures. T means the temperature and the numbers following T indicates the temperature level. D indicates the DLI and the numbers following D represent the DLI value.

Treatment	T30/D11	T30/D23	T35/D11	T35/D23	T40/D11	T40/D23
PPFD (μmol/m^2/s)	218	456	218	456	218	456
DLI (μmol/m^2/d)	11	23	11	23	11	23
Temperature (°C)	30	30	35	35	40	40

Growth measurements

Plant growth parameters, including shoot length (cm) and leaf size (width and length in cm), as well as the number of leaves were measured weekly from five plants per treatment. At the end of the experimental period i.e. after 9 weeks of cultivation under various growth conditions,

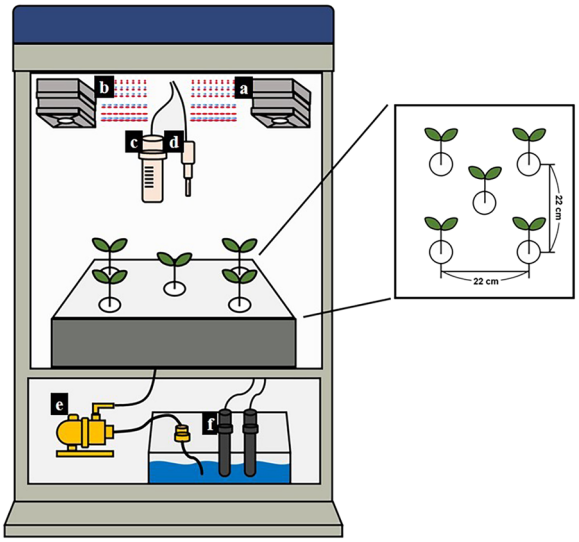

Fig. 1 Plant density and cultivation system configuration. It consisted of (**a**) floating fan, (**b**) LED lamps (KLB-40-2C; KAST Engineering, Gumi, South Korea) consisting of 11 (white LED):4 (blue LED, 454 nm):7 (red LED, 658 nm) (**c**) CO_2 sensor module (KCD-HP100, Korea Digital Co., LTD, Seoul, South Korea) and (**d**) temperature and humidity sensor module (KSH-7310, Korea Digital Co., LTD, Seoul, South Korea), (**e**) water pump (Diaphragm Pump, GOOD PUMPs Co., LTD, Gangneung, South Korea), and (**f**) EC meter

plants that had been subjected to different treatments for five weeks were harvested, and their fresh shoot and root weights (grams) were measured.

Sample preparation for HPLC–DAD analysis

The basil shoot samples were freeze-dried at minus 80 °C for one week and grounded into fine powder using an IKA® A11 basic mill (IKA-Werke, Staufen, Germany). For extraction purpose, 500 mg of lyophilized basil powder was mixed with 40 mL of 70% ethanol. The mixture was sonicated at 60 °C in an ultrasonic water bath (UCP-10, Lab companion, Korea) for 1 h, followed by centrifugation at 3500 rpm for 15 min. The supernatant extracts were filtered through a 0.45 µm filter (Smartpor-II, PTFE syringe filter) and then evaporated using a nitrogen concentrator (Allsheng MD 200, Hangzhou Allsheng Instrument Co., Ltd., Hangzhou, China). The resulting dried crude concentrates were re-dissolved in dimethyl sulfoxide (DMSO) and filtered through a 0.2 µm filter (Whatman, PVDF syringe filter) before HPLC–DAD analysis.

Determination of total phenolics content (TPC)

TPC was determined using the Folin-Ciocalteu method with some modification [33], with gallic acid (Sigma Aldrich, St. Louis, MO) as quantification standard. To create a calibration curve, the same reaction was conducted with gallic acid at concentrations ranging from 40 to 500 µg/mL, and the results were expressed as milligrams of gallic acid equivalent (mg GAE) per gram of dry weight (DW). In sample preparation, 10 mg/mL of the samples was mixed with 2% Na_2CO_3 for 3 min. Afterward, 10 µL of 1 N Folin-Ciocalteu reagent was added and allowed to react for 30 min at room temperature. The absorbance of the samples at 750 nm was measured using a multi-detection microplate reader, Synergy HT (BioTek Instruments, Winooski, VT, USA).

Quantification of rosmarinic acid content (RAC)

RAC was quantified using an Agilent 1260 Infinity HPLC system (Agilent Technologies) equipped with a diode array detector (DAD). RA in basil extracts was separated using a YMC Triart C18 column (4.6 × 250 mm, 5 µm; YMC Co.) with the oven temperature maintained at 40 °C. The mobile phases consisted of 0.2% formic acid in water (A) and acetonitrile (B), and the gradient program for the mobile phase was as follows: 0–4 min, 0–20% (B); 4–10 min, 20–37% (B); 10–15 min, 37% (B); 15–18 min, 37–60% (B). The injection volume was 10 µL, and the flow rate was 1 mL/min. RA was detected at 330 nm. For the generation of the standard curve, RA (PubChem CID: 639,655) was purchased from Sigma-Aldrich (St. Louis, USA). RA eluted at a retention time of 11.94 min, and eight concentrations of RA (ranging from 5 to 200 µg/mL) were prepared by diluting with methanol to create the calibration curve ($Y = 34.912X–64.669$, $R^2 = 0.999$).

Determination of antioxidant activities

The antioxidant activities of basil extracts were determined by measuring 2,2-diphenyl-1-picrylhydrazyl (DPPH) radical scavenging activity and 2,2'-azino-bis-(3-ethylbenzothiazoline 6-sulphonic acid) (ABTS) radical scavenging activity.

The DPPH radical scavenging activity was measured by previous method with some modifications [34]. Sample extracts (10 µL) were mixed with 190 µL of DPPH reagent, and the mixture was incubated for 30 min in the dark. The absorbance was then measured at 517 nm using a multi-detection microplate reader (Synergy HT, BioTek Instruments, Winooski, VT, USA). The ABTS radical scavenging activity was determined as described previously with some modifications [35]. The ABTS radical scavenging activity was determined by mixing 190 µL of $ABTS^+$ solution with 10 µL of sample extracts, also in the dark. The absorbance was measured at 734 nm after 10 min using the same microplate reader. The RC_{50} value, representing the concentration of the sample required to reduce the initial radical concentration by 50%, was calculated and expressed in µg/mL.

Profiling of VOCs by HS-SPME-GC-TOF–MS

VOCs analysis was performed following an established protocol [36] using head space (HS)-solid phase microextraction (SPME) coupled with GC-TOF–MS (LECO Pegasus GC HRT, Leco Corp., St. Joseph, MI, USA). The freeze-dried basil was finely ground, and 20 mg of basil was mixed with 1 mL of a saturated 30% NaCl solution, with 2 µL of 0.2 mg/mL 3-pentanol serving as the internal standard. Sampling was done using an SPME holder equipped with a 50/30 µm fiber (DVB/CAR/PDMS, model 57,348-U, Supelco, Bellefonte, PA, USA). Prior to use, the fiber was conditioned at 250 °C for 5 min. VOCs were then extracted through the SPME fiber at 70 °C with a stirring rate of 500 rpm for 20 min. Subsequently, GC-TOF–MS analysis was performed on a capillary column (Rtx-5MS, 30 m length, 0.25 mm diameter, 0.25 µm thickness, 5% diphenyl, 95% dimethyl polysiloxane, Restek, PA, USA) under a split mode (30:1). The front inlet and transfer line temperatures were set at 240 °C and 250 °C, respectively. The mass range covered 36 to 450 m/z. The ion source temperature was maintained at 250 °C with an ionization voltage of 70 eV, and helium was used as the carrier gas at a flow rate of 3 mL/min. The oven temperature program was set as follows: 60 °C for 1 min, followed by 150 °C at a rate of 13 °C/min, and then 180 °C at a rate of 8 °C/min. Subsequently, the temperature was programmed to increase to 200 °C at a rate of 10 °C/min and then further to 245 °C at a rate of 30 °C/min. Finally, it was held at 245 °C for 3 min. The relative quantity of VOCs was calculated based on the concentration of the internal standard. Retention indices (RI) were determined from the retention times of a series of n-alkanes (saturated C7–C40) using linear interpolation. The VOCs were identified based on RI and compared with the recorded mass spectra of each compound using a mass spectrum library search (NIST).

Profiling of primary metabolite through GC-TOF–MS

To extract and derivatize the primary metabolites, 50 mg of freeze-dried basil samples were mixed with 1 mL of a solvent mixture (chloroform/methanol/water, 1:2.5:1, *v/v/v*), with the addition of ribitol (0.2 mg/mL) as an internal standard [37]. The mixture was sonicated at 37 °C in an ultrasonic water bath (UCP-10, Lab companion, Korea) for 30 min and then centrifuged at 13,000 rpm for 5 min. After centrifugation, 500 µL of the supernatant was dried using a nitrogen concentrator, and the dried residue was mixed with 50 µL of methoxyamine hydrochloride (40 mg/mL in pyridine) and heated at 37 °C for 90 min. Subsequently, 50 µL of N-Methyl-N-(trimethylsilyl)-trifluoroacetamide (MSTFA) reagent was added for derivatization, followed by incubation at 37 °C for 30 min. Prior to analysis, the samples were filtered through a 0.2 µm PVDF syringe filter.

Analysis of primary metabolites in basil was performed using an Agilent 7890B GC coupled with a Pegasus HT TOF–MS (Leco Corporation, St. Joseph, MI, USA). Derivatized metabolites were separated on a RESTEK Rtx-5MS column (30 m × 0.25 mm I.D., 0.25 µm film thickness), and helium gas was used as the carrier gas at a constant flow rate of 1 mL/min. The oven temperature was initially set at 80 °C for 2 min, and then increased to 180 °C at a rate of 10 °C/min. It was further programmed to reach 200 °C at a rate of 2 °C/min and then increased at a rate of 12 °C/min up to 300 °C, where it was held for 2 min. The ion source and transfer line temperatures were set at 200 °C and 250 °C, respectively. The injection volume of the sample was 1 µL in split mode (30:1, v/v), and the mass scan range covered 24–500 m/z. Five biological replicates were prepared for each sample, and the relative quantity and identification of primary metabolites were determined using the same method as for VOCs.

Statistical analysis

Descriptive statistics for the studied characteristics were presented as mean ± standard deviation. ANOVA (Analysis of Variance) was performed to determine whether there was a difference between the groups in terms of considered characteristics. Post-hoc Tukey's Honestly Significant Difference (HSD) test was used to determine significant differences. Statistical significance level was considered as 5% ($p < 0.05$) and R Studio was used for all statistical computations. Heatmap analysis was conducted using MetaboAnalyst V5.0. Each treatment comprised five replications.

Results

Influence of elevated temperature and light on growth attributes of Basil

In this study, the growth parameters exhibited a steady increase during the cultivation period, with differences becoming more pronounced across all parameters as the growth progressed (Table 1). Shoot length did not show significant differences until 58 days after sowing (DAS). However, at 65 DAS, a significant difference was observed ($p < 0.05$). Notably, under normal conditions (T30), there was a positive correlation between shoot length and the increase in daily light integral (DLI). In contrast, changes in DLI had no significant effect on shoot length under mild and extreme temperature stresses (T35 and T40). Moreover, significantly larger leaf area indicators (leaf length and width) were observed in T30 under the same DLI levels, and these measurements showed a moderate positive correlation with internode length ($r = 0.4272$

Table 1 Growth attributes of Basil cultivated under elevated temperatures and DLI

Growth Parameters	DAS	T30		T35		T40	
		D11	D23	D11	D23	D11	D23
Shoot length (cm)	30	3.3 ± 0.5a	3.5 ± 0.2a	3.2 ± 0.4a	3.4 ± 0.3a	3.5 ± 0.3a	3.4 ± 0.4a
	37	6.4 ± 1.3a	6.4 ± 0.5a	6.7 ± 0.9a	7.6 ± 1.8a	7.1 ± 1.8a	8.0 ± 1.4a
	44	15.9 ± 2.2a	17.4 ± 1.6a	16.2 ± 2.4a	15.5 ± 4.4a	12.0 ± 4.0a	16.1 ± 2.5a
	51	23.6 ± 1.8ab	25.3 ± 0.7ab	24.4 ± 3.8ab	26.6 ± 2.1a	20.8 ± 4.9b	23.2 ± 1.9ab
	58	30.6 ± 2.1a	35.4 ± 5.9a	33.3 ± 5.3a	32.4 ± 8.0a	27.6 ± 5.7a	27.1 ± 2.0a
	65	35.5 ± 1.8abc	43.0 ± 5.9a	40.6 ± 5.7ab	39.8 ± 8.5abc	31.6 ± 6.3bc	29.3 ± 1.8c
Leaf length (cm)	30	3.6 ± 0.3a	3.6 ± 0.3a	3.6 ± 0.2a	3.5 ± 0.3a	3.3 ± 0.4a	3.4 ± 0.3a
	37	5.6 ± 1.0a	5.2 ± 0.5a	5.0 ± 0.5a	5.6 ± 0.7a	4.8 ± 1.0a	4.9 ± 0.9a
	44	9.6 ± 1.4a	7.6 ± 0.8b	6.5 ± 0.5b	6.8 ± 0.5b	7.2 ± 1.4b	6.6 ± 0.9b
	51	11.9 ± 0.6a	8.9 ± 1.6b	9.2 ± 1.0b	8.0 ± 0.5bc	9.1 ± 1.7b	6.5 ± 0.9c
	58	12.1 ± 1.6a	9.3 ± 1.1b	8.7 ± 0.4bc	8.2 ± 0.4bc	9.2 ± 0.7b	7.0 ± 1.1c
	65	12.9 ± 1.0a	9.8 ± 1.5b	9.2 ± 1.3bc	8.7 ± 0.3bc	9.5 ± 0.6b	7.1 ± 1.3c
Leaf width (cm)	30	2.4 ± 0.5a	2.2 ± 0.1a	2.2 ± 0.2a	2.3 ± 0.3a	2.2 ± 0.4a	1.9 ± 0.2a
	37	3.9 ± 0.7ab	3.9 ± 0.3a	3.7 ± 0.5ab	2.9 ± 0.7bc	2.9 ± 0.5abc	2.6 ± 0.4c
	44	5.6 ± 0.4a	4.4 ± 0.3b	3.5 ± 0.5b	3.5 ± 0.5b	3.8 ± 0.7b	3.5 ± 0.6b
	51	5.8 ± 0.6a	4.5 ± 0.4bc	5.0 ± 0.5ab	3.9 ± 0.4 cd	4.4 ± 0.4bc	3.3 ± 0.6d
	58	6.5 ± 0.8a	4.7 ± 0.7b	4.7 ± 0.4b	4.0 ± 0..2b	4.5 ± 0.3b	4.2 ± 0.5b
	65	6.5 ± 0.9a	5.1 ± 0.4b	4.9 ± 0.4b	4.3 ± 0.2b	4.8 ± 0.4b	3.9 ± 1.3b
Leaf number (ea)	30	6.6 ± 0.9a	6.8 ± 0.8a	6.8 ± 0.8a	6.8 ± 0.8a	6.4 ± 0.9a	6.8 ± 0.8a
	37	17.6 ± 3.6b	25.2 ± 2.3ab	19.6 ± 2.2b	36.0 ± 14.4a	19.6 ± 9.0b	24.8 ± 7.6ab
	44	43.2 ± 6.8b	55.8 ± 14.8ab	45.6 ± 9.4b	93.8 ± 32.3a	66.0 ± 20.3ab	97.2 ± 37.3a
	51	82.4 ± 14.4c	125.4 ± 32.6bc	88.8 ± 30.7c	216.0 ± 77.8ab	139.6 ± 40.0ab	248.0 ± 60.5a
	58	120.4 ± 21.7c	224.4 ± 56.6bc	147.6 ± 27.9c	372.4 ± 135.7ab	244.8 ± 58.5abc	392.2 ± 114.1a
	65	133.2 ± 33.8d	343.6 ± 118.5abc	191.6 ± 47.2 cd	429.6 ± 151.3ab	277.8 ± 70.3bcd	472.0 ± 103.3a
Internode length (cm)		4.9 ± 0.5a	4.9 ± 0.6a	5.3 ± 1.0a	1.9 ± 0.2b	2.5 ± 0.6b	2.7 ± 0.3b
Root weight (g)		39.6 ± 8.65b	66.6 ± 19.0ab	51.0 ± 12.1b	91.2 ± 22.7a	49.0 ± 9.2.5b	51.2 ± 11.1b
Shoot weight (g)		46.4 ± 9.29b	68.4 ± 17.9ab	49.2 ± 9.26b	81.0 ± 25.5a	57.0 ± 16.9ab	39.2 ± 9.28b

Each treatment comprised five replicates and average of three for internodes. Values are the means ± standard deviation. Same lower cases represent non-significant difference and different lower cases (a–d) in the same row represent statistically significant differences among the groups according to Tukey HSD Test ($p < 0.05$). DAS, days after sowing

and 0.5008) (Fig. 2). Temperature and DLI also had an impact on production. Under T30 and T35, production increased with rising DLI. However, at extreme temperature stress (T40), high light intensity (D23) resulted in a slight decrease in yield. These observations indicated distinct morphological and yield changes resulting from long-term treatments of DLI and temperature.

Analysis of TPC and RAC under elevated temperature and light

The rosmarinic acid (RA) was identified as the major component in the basil used in this experiment, as presented in Additional file 1: Fig. S1. We observed that RAC significantly contributed to TPC, and a similar trend between RAC and TPC was evident, with a very high correlation coefficient (r) of 0.959 ($p < 0.05$) determined. When averaged across temperatures (Fig. 3A, B), it was found that TPC and RAC were higher at lower temperatures, with significantly higher values observed in T30 (TPC, 62.2 mg GAE/g; RAC, 37.0 mg/g) compared to T35 (TPC, 52.8 mg GAE/g; RAC, 29.0 mg/g) and T40 (TPC, 37.6 mg GAE/g; RAC, 13.0 mg/g). Overall, the effect of DLI on TPC (D11, 62.9 mg GAE/g; D23, 61.6 mg GAE/g) and RAC (D11, 38.9 mg/g; D23, 35.1 mg/g) was insignificant under T30 (Fig. 3B, D).

Status of VOCs under elevated temperature and light

We detected 44 VOCs that included 5 phenylpropenes, 16 monoterpenes, 15 sesquiterpenes, 5 aldehydes, and 3 other compound groups (Table 2). Linalool (monoterpene) and eugenol (phenylpropene) were identified as the major constituents of VOCs in basil, as displayed in Additional file 1: Fig. S2. Among the other components, relatively major compounds accounting for more than 1% on average were (E)-α-bergamotene (4.4%), eucalyptol (6.5%), α-terpineol (3.1%), and epi-α-cadinol

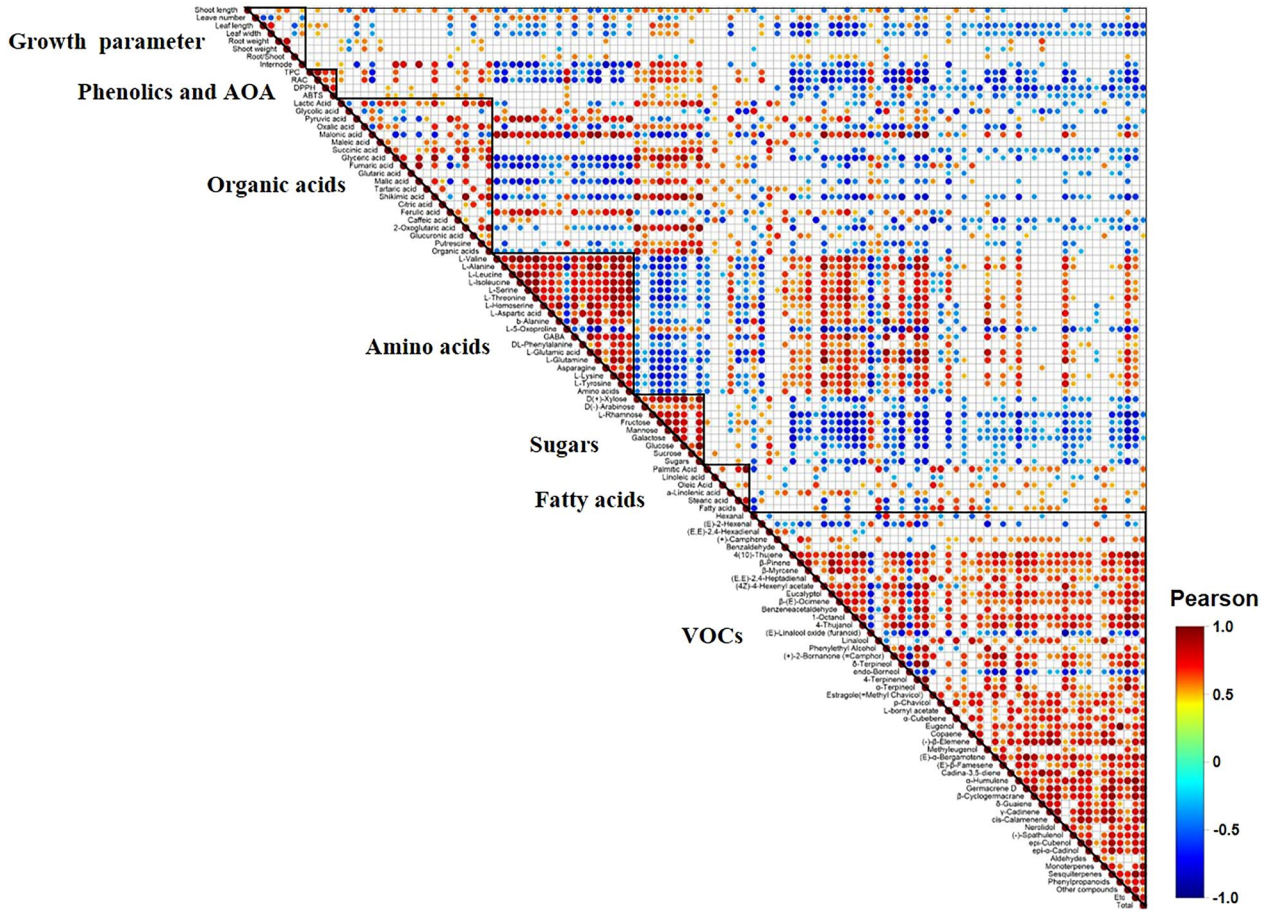

Fig. 2 Heatmap plot representing the correlation matrix between variables. It was constructed by diverse variables related to growth parameters [9], phenolics and antioxidant activities [4], organic acids [20], amino acids [18], sugars [9], fatty acids [6], and VOCs [50]. Significance levels were expressed using numbers for significant results ($p < 0.05$) and blanks for non-significant result. Positive correlations were depicted in red, while negative correlations were shown in blue, as indicated by the color scale bar located at the right of the heatmap

(2.5%) and their quantification results were presented in Fig. 4. However, the distribution of total VOCs content, ranging from 163.8 µg/20 mg to 394.3 µg/20 mg, was determined by two main constituents (linalool and eugenol), which accounted for 26.2% and 48.1% on average. Under the lowest temperature condition (T30), a high DLI had a positive effect on phenolic compounds (TPC and RAC) as shown in Fig. 1, however had a negative effect on VOCs, as indicated in Table 3. Meanwhile, temperature stress-induced conditions (T35 and T40) and the lowest DLI (D11) stimulated VOCs production (Fig. 4). The highest content was observed in T35/D11 (361.9 ± 33.7 µg/20 mg), followed by T35/D23 (305.3 ± 25.7 µg/20 mg) and T40/D11 (293.4 ± 27.9 µg/20 mg). These opposite trends resulted in a negative correlation between the main VOCs, including linalool, eugenol, eucalyptol, (E)-α-bergamotene, α-terpineol, and epi-α-cadinol, with TPC (r = 0.1860, −0.4271, −0.6910, −0.5997, −0.7479, and −0.3415, respectively) and RAC (r = 0.2366, −0.4271, −0.7481, −0.6196, −0.8166, and −0.4138, respectively), as presented in Fig. 2.

Analysis of antioxidant activities

DPPH and ABTS radical assays have been developed to spectrophotometrically monitor antioxidant activities as such assays are considered effective for screening and identifying the natural bioactivity of complex mixtures. We recorded higher activity in the ABTS assay (RC50 = 65.7 ± 15.8 µg/mL) compared to the DPPH assay (RC50 = 133.2 ± 3.2 µg/mL) as shown in Fig. 3. Notably, temperature was found a significant factor in antioxidant activity. Based on the temperature grouping (Fig. 3C, D), the T30 treatment exhibited stronger DPPH (RC50 = 107.1 ± 19.4 µg/mL) and ABTS radical scavenging activities (RC50 = 55.2 ± 5.7 µg/mL) compared to T35 (DPPH RC50 = 141.6 ± 29.7 µg/

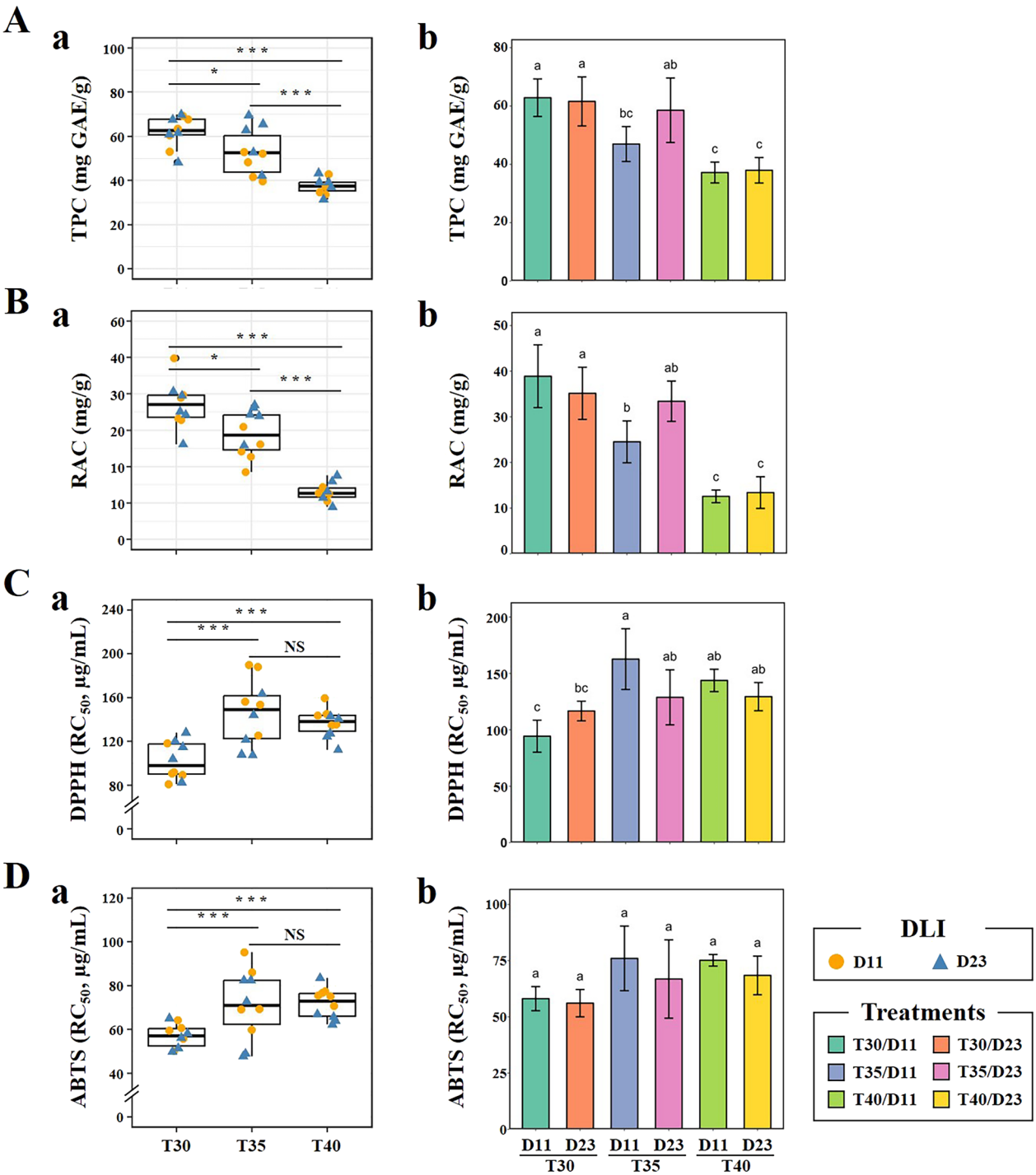

Fig. 3 Effects of temperature and DLI on the TPC, RAC, and antioxidant activities. **A** TPC (mg GAE/g), **B** RAC (mg/g), **C** DPPH radical scavenging activity (RC50; μg/mL), and **D** ABTS radical scavenging activity (RC50; μg/mL) were expressed based on temperature grouping (**a**) and within each group (**b**). In box-plots, each group consisted of five biological replicates represented by individual scores, and different light conditions were indicated by color (D11, orange; D23, blue). Statistical differences between temperature groups were determined using Student's T-test (*$p < 0.05$; ***$p < 0.005$; NS, non-significant). The bar graph represents the means ± standard deviation of five biological replicates in each group, and non-significant differences are indicated by the same letters according to Tukey HSD Test ($p < 0.05$)

Table 2 HS-SPME-GC-TOF–MS analysis for VOCs profiling and dynamic changes of basil

Compound name	T30		T35		T40	
	D11	D23	D11	D23	D11	D23
Phenylpropenes						
Benzaldehyde	0.1 ± 0.0bc	0.1 ± 0.0a	0.1 ± 0.0c	0.1 ± 0.0ab	0.1 ± 0.0a	0.1 ± 0.0bc
Estragole	ND	ND	0.1 ± 0.0a	0.0 ± 0.0c	0.0 ± 0.0c	0.0 ± 0.0b
ρ-Chivacol	0.2 ± 0.1b	0.2 ± 0.0b	0.5 ± 0.1a	0.4 ± 0.1a	0.2 ± 0.1b	0.2 ± 0.0b
Eugenol	115.6 ± 16.9b	112.4 ± 13.2b	144.9 ± 11.5a	132.3 ± 15.5ab	147.4 ± 15.4a	133.6 ± 10.0ab
Methyl eugenol	0.5 ± 0.1d	1.5 ± 0.3bc	1.5 ± 0.5b	0.6 ± 0.1 cd	2.3 ± 0.9b	3.9 ± 0.3a
Total	116.5 ± 17.0b	114.2 ± 13.2b	147.1 ± 11.6a	133.4 ± 15.6ab	150.0 ± 15.4a	137.7 ± 10.3ab
Monoterpenes						
(+)-Camphene	ND	0.0 ± 0.0 a	0.0 ± 0.0 ab	0.0 ± 0.0 b	0.0 ± 0.0 b	0.0 ± 0.0 b
Thujene	0.0 ± 0.0c	0.0 ± 0.0c	0.1 ± 0.0ab	0.1 ± 0.0b	0.2 ± 0.0ab	0.2 ± 0.0a
β-pinene	0.0 ± 0.0d	0.3 ± 0.0c	0.3 ± 0.0ab	0.3 ± 0.1bc	0.4 ± 0.0ab	0.4 ± 0.0a
β-Myrcene	0.0 ± 0.0d	0.1 ± 0.0bc	0.1 ± 0.0c	0.2 ± 0.0abc	0.2 ± 0.0ab	0.2 ± 0.0a
Eucalyptol	5.7 ± 1.3d	15.7 ± 5.6c	21.1 ± 3.1abc	19.0 ± 1.8bc	25.6 ± 3.9a	24.2 ± 0.7ab
β-(E)-Ocimene	0.0 ± 0.0c	0.2 ± 0.1b	0.2 ± 0.0b	0.4 ± 0.1a	0.4 ± 0.1a	0.4 ± 0.1a
Thujanol	0.2 ± 0.0c	0.2 ± 0.0c	0.5 ± 0.1a	0.4 ± 0.0b	0.6 ± 0.1a	0.5 ± 0.1a
(E)-Linalool oxide	0.1 ± 0.0a	0.1 ± 0.0ab	0.1 ± 0.0bc	0.1 ± 0.0bc	0.0 ± 0.0d	0.1 ± 0.0c
Linalool	39.4 ± 4.5c	91.1 ± 10.6b	122.5 ± 14.5a	96.2 ± 8.7b	46.6 ± 7.3c	51.6 ± 6.5c
Camphor	0.3 ± 0.1 cd	0.2 ± 0.0d	1.5 ± 0.2a	0.4 ± 0.1c	1.4 ± 0.1ab	1.2 ± 0.1b
δ-Terpineol	1.2 ± 0.3c	1.0 ± 0.1c	1.9 ± 0.1b	1.8 ± 0.2b	3.2 ± 0.2a	3.2 ± 0.3a
endo-Borneol	2.0 ± 0.2a	1.3 ± 0.2b	0.3 ± 0.0 cd	1.9 ± 0.2a	0.2 ± 0.0d	0.5 ± 0.1c
4-Terpineol	0.1 ± 0.0c	0.1 ± 0.0bc	0.1 ± 0.0bc	0.2 ± 0.0b	0.3 ± 0.0a	0.4 ± 0.0a
α-Terpineol	4.3 ± 0.7c	4.3 ± 0.7c	7.6 ± 0.4b	7.5 ± 0.3b	13.2 ± 1.0a	14.5 ± 1.5a
L-bornyl acetate	0.9 ± 0.1d	1.5 ± 0.4 cd	2.0 ± 0.6bc	3.8 ± 0.4a	3.8 ± 0.7a	2.5 ± 0.3b
(E)-α-Bergamotene	3.6 ± 0.7d	5.8 ± 1.0d	23.7 ± 3.8a	11.9 ± 1.1c	17.4 ± 1.8b	15.2 ± 0.9bc
Total	57.9 ± 5.1d	122.0 ± 10.7bc	182.2 ± 18.8a	144.0 ± 10.0b	113.4 ± 12.2c	115.1 ± 9.4c
Sesquiterpenes						
α-Cubebene	0.0 ± 0.0c	0.0 ± 0.0bc	0.1 ± 0.0a	0.1 ± 0.0ab	0.0 ± 0.0c	0.0 ± 0.0c
Copaene	0.1 ± 0.0d	0.1 ± 0.0bc	0.2 ± 0.0a	0.1 ± 0.0b	0.1 ± 0.0 cd	0.1 ± 0.0 cd
(−)-β-Elemene	0.3 ± 0.1e	0.5 ± 0.1de	1.4 ± 0.3a	1.2 ± 0.1ab	1.0 ± 0.2bc	0.8 ± 0.1 cd
(E)-β-Famesene	0.3 ± 0.1b	0.4 ± 0.1b	1.0 ± 0.1a	0.4 ± 0.1b	0.9 ± 0.1a	1.0 ± 0.1a
Cadina-3,5-diene	0.1 ± 0.0d	0.2 ± 0.0 cd	0.3 ± 0.1b	0.5 ± 0.1a	0.3 ± 0.1bc	0.2 ± 0.0d
α-Humulene	0.7 ± 0.1d	1.4 ± 0.2d	3.7 ± 0.5bc	3.3 ± 0.2c	4.9 ± 0.4a	4.2 ± 0.6b
Germacrene D	0.6 ± 0.1d	1.8 ± 0.3c	4.6 ± 1.0a	2.7 ± 0.6bc	3.0 ± 0.2b	2.9 ± 0.4b
β-Cyclogermacrane	0.3 ± 0.1c	0.9 ± 0.0c	2.6 ± 0.3a	2.1 ± 0.8ab	2.1 ± 0.2ab	1.7 ± 0.1b
δ-Guaiene	ND	0.3 ± 0.0 c	0.5 ± 0.1 b	0.9 ± 0.0 a	0.5 ± 0.1 b	0.2 ± 0.0 c
γ-Cadinene	0.8 ± 0.1d	1.8 ± 0.3 cd	4.0 ± 1.2a	3.5 ± 0.4ab	2.7 ± 0.4bc	2.2 ± 0.2c
cis-Calamenene	0.3 ± 0.1d	0.4 ± 0.1 cd	0.8 ± 0.1a	0.8 ± 0.1ab	0.6 ± 0.2bc	0.5 ± 0.1c
Nerolidol	0.2 ± 0.0e	0.2 ± 0.0de	0.4 ± 0.1bc	0.3 ± 0.1 cd	0.8 ± 0.1a	0.5 ± 0.1b
(−)-Spathulenol	0.8 ± 0.1c	0.7 ± 0.1c	1.6 ± 0.5a	1.1 ± 0.1bc	1.5 ± 0.1ab	1.4 ± 0.1ab
epi-Cubenol	0.5 ± 0.1b	0.5 ± 0.1b	0.9 ± 0.2a	1.0 ± 0.2a	0.9 ± 0.2a	0.7 ± 0.0ab
epi-α-Cadinol	4.6 ± 1.3c	5.7 ± 0.8bc	8.4 ± 1.9a	8.1 ± 1.0ab	8.8 ± 1.6a	6.6 ± 0.5abc
Total	9.5 ± 1.8c	15.0 ± 1.8c	30.7 ± 5.9a	26.0 ± 2.4ab	28.1 ± 3.1ab	23.0 ± 1.7b
Aldehydes						
Hexanal	0.0 ± 0.0a	0.0 ± 0.0b	0.0 ± 0.0b	0.0 ± 0.0bc	0.0 ± 0.0c	0.0 ± 0.0c
(E)-2-Hexenal	0.8 ± 0.1a	0.5 ± 0.1c	0.6 ± 0.1b	0.8 ± 0.1ab	0.4 ± 0.1c	0.3 ± 0.0c
(E,E)-2,4-Hexadienal	0.0 ± 0.0d	0.3 ± 0.0a	0.1 ± 0.0c	0.0 ± 0.0d	0.1 ± 0.0b	0.0 ± 0.0d
(E,E)-2,4-Heptadienal	0.3 ± 0.0 cd	0.3 ± 0.0d	0.6 ± 0.1a	0.4 ± 0.1bc	0.4 ± 0.1bcd	0.5 ± 0.1b
Benzeneacetaldehyde	0.1 ± 0.0d	0.1 ± 0.0c	0.1 ± 0.0d	0.2 ± 0.0b	0.3 ± 0.0a	0.3 ± 0.0a

Table 2 (continued)

Compound name	T30		T35		T40	
	D11	D23	D11	D23	D11	D23
Total	1.2 ± 0.1ab	1.1 ± 0.1b	1.4 ± 0.1a	1.4 ± 0.1a	1.1 ± 0.2b	1.2 ± 0.1b
Etc						
(4Z)-4-Hexenyl acetate	ND	ND	ND	ND	0.1 ± 0.0 a	0.1 ± 0.0 b
1-Octanol	0.2 ± 0.0b	0.2 ± 0.0b	0.4 ± 0.1a	0.5 ± 0.1a	0.5 ± 0.0a	0.5 ± 0.1a
Phenylethyl Alcohol	ND	ND	ND	ND	0.1 ± 0.0 a	0.1 ± 0.0 b
Total	0.2 ± 0.0c	0.2 ± 0.0c	0.4 ± 0.1b	0.5 ± 0.1b	0.7 ± 0.0a	0.7 ± 0.1a
Total VOCs	185.3 ± 21.2d	252.5 ± 23.0c	361.7 ± 33.7a	305.3 ± 25.7b	293.4 ± 27.9bc	277.8 ± 20.3bc

Experiment was conducted five biological replications and data were expressed as μg/20 mg (means ± standard deviation). Same lower cases represent non-significant difference and different lower cases (a–d) in the same row represent statistically significant differences among the groups according to Tukey HSD Test ($p < 0.05$)

mL; ABTS RC50 = 66.3 ± 16.3 μg/mL) and T40 (DPPH RC50 = 150.9 ± 29.3 μg/mL; ABTS RC50 = 75.5 ± 16.3 μg/mL).

Under the same DLI conditions, higher activity was observed at lower temperatures, and this temperature-dependent trend became more pronounced at lower DLI levels, regardless of the experimental method. Therefore, strong correlations ($p < 0.0001$) were observed between phenolic contents and antioxidant activities (Fig. 2), as follows: TPC-DPPH: r = 0.6666; TPC-ABTS: r = 0.6632; RAC-DPPH: r = 0.5960; and RAC-ABTS: r = 0.5803. Considering the results categorized by temperature conditions, the highest functional value, as judged by TPC, RAC, and antioxidant activities of basil grown under T30 conditions, was clearly demonstrated.

ANOVA analysis

A two-way ANOVA analysis was performed to evaluate the effects of variables (temperature and DLI) on growth patterns, secondary metabolites (TPC, RAC, and VOCs), and antioxidant activities. While the production based on shoot weight was significantly influenced by the combination of temperature and DLI, not by single factors, a significant effect of temperature was observed in most cases ($p < 0.05$). In particular, a highly significant effect of temperature on TPC, RAC, and total VOCs was determined ($p < 0.005$). TPC and RAC showed a p value of less than 0.005 only with temperature as a factor, but total VOCs significantly changed with temperature alone and when combined with DLI.

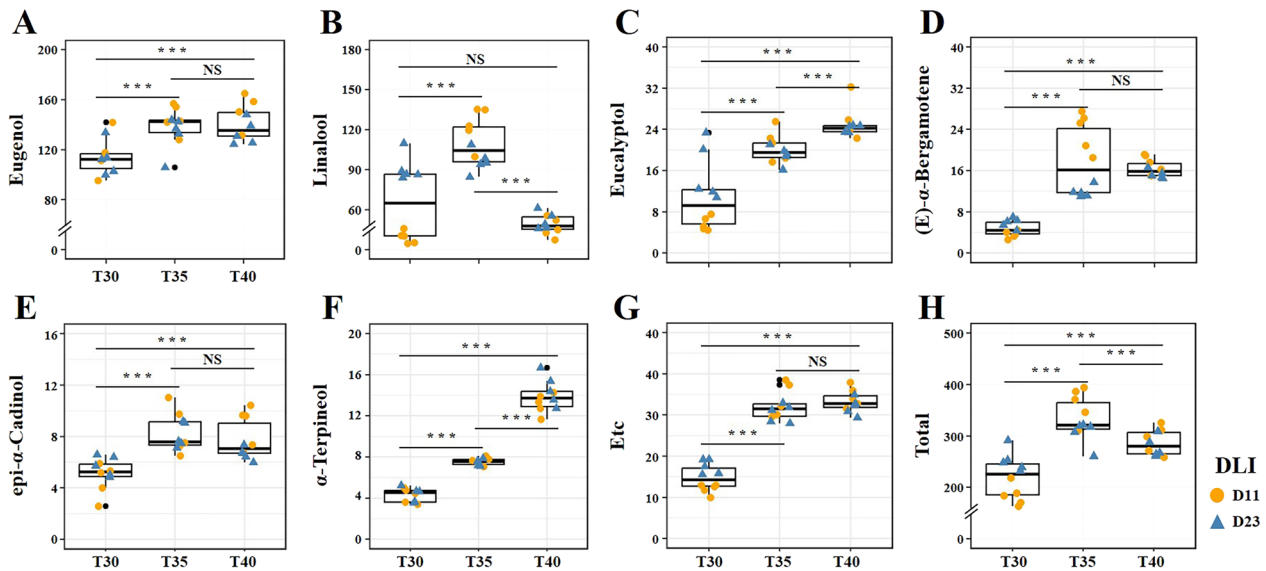

Fig. 4 Content (μg/g) of main compositions of VOCs. **A** Eugenol, **B** linalool, **C** eucalyptol (**C**), (**E**)-α-bergamotene(**D**), epi-α-cadinol (**E**), α-terpineol (**F**), etc. (**G**), and total VOCs (**H**) in basil were analyzed using HS-SPME-GC-ToF–MS. In box-plots, each group consisted of five biological replicates represented by individual scores and different light conditions were indicated by color (D11, orange; D23, blue). Statistical differences between temperature groups were determined using Student's T-test. ***$p < 0.005$; NS, non-significant

Table 3 Summary table of two-way (factorial) ANOVA

Variable	Source	df	SS	MS	F	p-value	
Shoot length	T	2	580.3	2090.15	9.419	< 0.005	***
	DLI	1	15.8	15.84	0.514	0.4802	NS
	T * DLI	2	137.3	68.64	2.228	0.1295	NS
Leave number	T	2	93,265	46,633	5.001	0.0153	*
	DLI	1	344,112	344,112	36.903	< 0.0005	***
	T * DLI	2	2452	1226	0.131	0.8774	NS
Leaf length	T	2	50.76	25.380	21.445	< 0.0005	***
	DLI	1	30.00	30.000	25.349	< 0.0005	***
	T * DLI	2	9.12	4.561	3.854	0.0354	*
Leaf width	T	2	11.605	5.802	11.194	< 0.0005	***
	DLI	1	7.400	7.400	14.277	< 0.0005	***
	T * DLI	2	0.889	0.444	0.857	0.4369	NS
Root weight	T	2	2580	1290	5.924	< 0.0005	***
	DLI	1	4014	4014	18.432	< 0.0005	***
	T * DLI	2	1861	931	4.273	0.0258	*
Shoot weight	T	2	1631	815.6	3.183	0.0594	NS
	DLI	1	963	963.3	3.759	0.0644	NS
	T * DLI	2	3755	1877.4	7.327	< 0.0005	***
Root-Shoot ratio	T	2	0.2899	0.1450	4.672	0.1934	NS
	DLI	1	0.5018	0.5018	16.171	< 0.0005	***
	T * DLI	2	0.2680	0.1340	4.318	0.0250	*
Internode length	T	2	27.299	13.650	35.460	< 0.0005	***
	DLI	1	8.501	8.501	22.080	< 0.0005	***
	T * DLI	2	20.602	10.301	26.760	< 0.0005	***
TPC	T	2	3088.8	1544.4	30.673	< 0.0005	***
	DLI	1	102.7	102.7	2.040	0.1660	NS
	T * DLI	2	239.2	119.6	2.376	0.1140	NS
RAC	T	2	2990.9	1495.4	66.832	< 0.0005	***
	DLI	1	29.8	29.8	1.330	0.2602	NS
	T * DLI	2	204.9	102.4	4.578	0.0207	*
DPPH	T	2	8895	4448	14.414	< 0.0005	***
	DLI	1	558	558	1.809	0.1912	NS
	T * DLI	2	4072	2036	6.599	0.0052	**
ABTS	T	2	1405.9	702.9	6.434	0.0058	**
	DLI	1	266.7	266.7	2.441	0.1313	NS
	T * DLI	2	66.4	33.2	0.304	0.7408	NS
Total VOCs	T	2	66,276	33,138	50.130	< 0.0005	***
	DLI	1	19	19	0.029	0.8660	NS
	T * DLI	2	19,872	9936	15.031	< 0.0005	***

Significance (*p*-value) of the independent variables temperature (T) and light intensity (DLI) and interaction effects on growth parameters, phytochemicals, and antioxidant activities. TPC, total phenolics content (mg GAE/g, DW); RAC, rosmarinic acid content (mg/g, DW); DPPH, RC_{50} value of DPPH radical scavenging activity (μg/mL); ABTS, RC50 value of ABTS radical scavenging activity (μg/mL); Total VOCs, total volatile compounds content (μg/10 mg); $*p < 0.05$; $**p < 0.01$; $***p < 0.005$; NS, non-significant

Profiling of primary metabolites

Based on the secondary metabolite analysis and two-way ANOVA, it was elucidated that temperature primarily regulates the secondary metabolism of basil. We also conducted an analysis of primary metabolites in this study. The variables within the same category (such as organic acids, amino acids, sugars, and fatty acids) displayed positive correlations with one another,

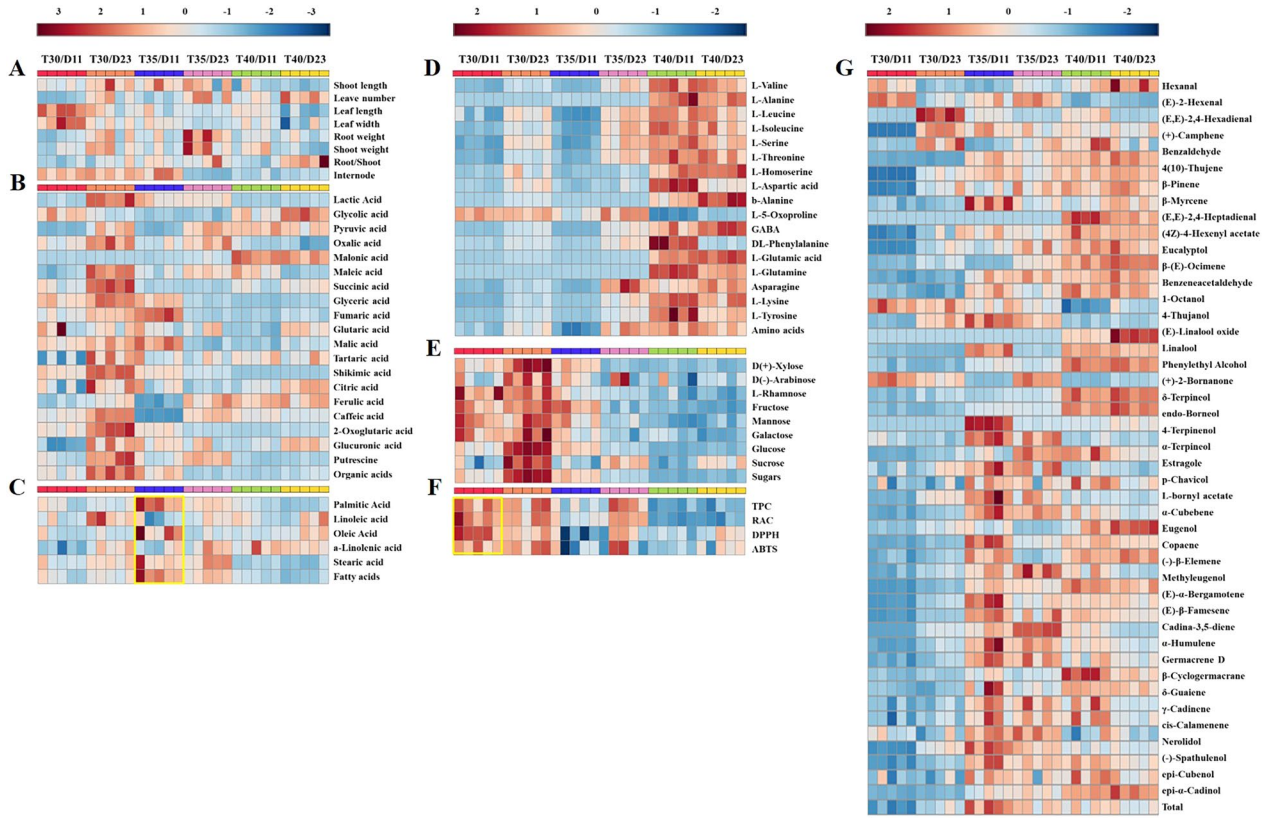

Fig. 5 Heatmap analysis between cultivation conditions and metabolites. Visulization was conducted un including (**A**) growth parameters, (**B**) organic acids, (**C**) fatty acids, (**D**) amino acids, (**E**) sugars, (**F**) phenolics and antioxidants, and (**G**) VOCs for each sample. The data were normalized, and a color-bar positioned above the heatmap indicated the Pearson correlation coefficient, with blue representing lower content and red representing higher content. Rows represented the variables, while columns represented the samples, which were color-coded according to the respective growth conditions: red for T30/D11, orange for T30/D23, blue for T35/D11, pink for T35/D23, green for T40/D11, and yellow for T40/D23

as indicated in Fig. 2. Furthermore, the results revealed that primary metabolites exhibited variations based on temperature, as illustrated in Fig. 5. Consequently, we averaged the results by temperature to facilitate interpretation. The total organic content and total sugar content decreased with rising temperatures, while the trend for total amino acids was the opposite. Notably, the highest total organic acids content was observed in the T30 condition (128.5 ± 21.3 μg/10 mg), which was approximately 1.17- and 1.29- times higher than the T35 (110.2 ± 16.2 μg/10 mg) and T40 (55.2 ± 16.4 μg/10 mg) conditions. The content of all observed organic acids (fumaric acid, malic acid, shikimic acid, and citric acid) related to the TCA cycle contributed significantly to the total organic acids content, with positive correlations (r = 0.7180, 0.8260, 0.8860, and 0.5643, respectively). In the T30 condition, it was observed that as DLI increased, the content of these organic acids and sugars also increased. Similarly, the total sugar content followed the same trend. T30 (90.5 ± 32.8 μg/10 mg) exhibited 1.64- and 3.64- times higher content compared to T35 (55.2 ± 16.4 μg/10 mg) and T40 (24.9 ± 3.5 μg/10 mg), respectively. Most sugar components, except for sucrose, displayed significantly positive correlations with total sugar content. In particular, glucose, which represented over 50% of the total sugar content, exhibited a very strong correlation with total sugar content (r value of 0.999). This is why the highest total sugar content was determined in T30/D23 (120.6 ± 8.0 μg/10 mg), where the glucose content was the highest (99.0 ± 6.9 μg/10 mg). Conversely, the total amino acids content exhibited a significant correlation within the total amino acids content. All detected amino acids, except for 5-oxoproline, showed positive correlations. The content of total amino acids was found to be 1.33 times higher in T40 (27.5 ± 2.2 μg/10 mg) compared to T30 (20.6 ± 2.7 μg/10 mg) and 1.32 times higher compared to T35 (20.8 ± 7.0 μg/10 mg).

Discussions

It is widely known that the preferred temperature range for most plant species typically falls within the range of 20 to 30 °C [38]. However, when plants are exposed to temperatures exceeding their optimal growth range by more than 5 °C, they experience stress, which triggers a variety of metabolic defense mechanisms and leads to the accumulation of secondary metabolites [39]. It's important to note that prolonged exposure to stressful conditions can lead to an acclimation process in plants. This acclimation results in increased stress tolerance, which is characterized by higher survival rates and enhanced production [3]. Therefore, there have been ongoing efforts to improve both production and functionality by modulating these factors. In this study, basil plants were subjected to elevated temperatures and light intensities (D11 and D23), and their responses were comprehensively analyzed through the evaluation of various metabolites, including both primary and secondary metabolites.

Plants within the Lamiaceae family, especially those with high levels of phenolic compounds, are considered valuable sources of natural substances for healthcare [40]. Basil, a member of the Lamiaceae family, contains various phenolic compounds such as caffeic acid, chicoric acid, caftaric acid, p-coumaric acid, and RA. The distribution of these phenolic compounds varies among basil species and cultivars [41, 42]. Among these compounds, RA has been identified as the most prevalent phenolic compound in sweet basil, as well as in other Lamiaceae species like thyme, marjoram, sage, rosemary, and lemon balm [43, 44]. RA content significantly influences the antioxidant properties of these plants, and a strong correlation has been found between phenolic content and antioxidant activities in various plant species [45, 46]. RA has also been reported to have various health-related properties, such as inducing melanogenesis, photoprotective effects, and anti-staphylococcus aureus and anti-inflammatory activities. These properties make RA valuable for industrial applications, such as in anti-acne products [47, 48]. Therefore, enhancing the content of RA in basil is crucial to make it more valuable with higher economic returns. Researchers have conducted various experiments to enhance the content of these substances in basil, including modifying cultivation conditions like drought stress, silver treatment, heat stress, and phytohormone treatments [49–52]. Basil exposed to temperature stress activates the accumulation of RA, which serves as a main component of the plant's defense mechanism [53]. These findings are consistent with the previous results, where the highest TPC and RAC were observed under specific temperature conditions (T30). According to factorial ANOVA analysis, temperature alone showed a significant effect on TPC and RAC, while the combination of temperature and DLI did not have a significant effect. For the metabolomics aspect, prior research has also suggested that light intensity does not significantly affect the content of certain compounds in basil [54, 55]. This is in line with previous results where DLI alone or combined with temperature did not have a significant impact on TPC and RAC. Additionally, the non-significant combined effect was consistent with the previously mentioned decreased complex influence in tomatoes [56]. Furthermore, the elevated temperature induced significant changes in the VOCs contents. VOCs have numerous functions, such as mediating plant-plant interactions, facilitating plant-pathogen communication, repelling insects through chemotaxis, and attracting pollinators by releasing pheromones [57]. The production of VOCs in plants is a metabolic activity that varies in composition and quantity depending on the function, developmental stage, genotypes, species, site of biosynthesis, and environmental conditions [58]. A similar previous conducted on the effect of drought stress severity on the biosynthesis of phenylpropanoids and essential oils in basil reported a decreased gene expression (C4H, cinnamate 4-hydroxylase) in the upstream biosynthesis pathway and an increased gene expression (EOMT, eugenol O-methyltransferase; CVOMT, chavicol O-methyltransferase) [59]. Additionally, Rezaie, Abdollahi Mandoulakani [60] described that prolonged cold stress (over 48 h) did not show any difference in their expression compared to untreated plants. These previous studies highlighted the effect of certain plant VOCs that can be released in response to various abiotic and biotic stresses. For basil, two phenylpropanoids (eugenol and methyl chavicol) and two terpenoids (1,8-cineole and linalool) have been reported as the major compounds determining its flavor [61]. In this study, the main VOCs emitted by basil plants were linalool (monoterpene) and eugenol (phenylpropene), and significantly higher VOCs content was observed at the specific temperature of T35 conditions.

Primary metabolism is involved in a complex defense system by interacting with secondary metabolites and participating in reactions against environmental stressors. This involvement occurs through the regulation of carbohydrates, proteins, and lipids in plants [62]. Due to differences in secondary metabolism responses to light and temperature treatments, an attempt was made to confirm the mechanism differences through primary metabolite analysis. Temperature stress has been reported to alter respiration and photosynthesis in plants, resulting in a shortened life cycle and decreased plant productivity [63]. It also affects the activity of enzymes involved in the carbon flux of the chloroplast stroma [64]. However, it should be noted that the impact of stress can vary depending on the

type, intensity, duration, and developmental stage of the plant [65]. In unstressed plants, normal photosynthetic processes occur, and glucose produced serves as an energy source through glycolysis [66]. However, when plants are exposed to photosynthetic stress, such as temperature stress, drought stress, or excessive light, the equilibrium between the production and scavenging of ROS is disrupted, leading to excessive ROS accumulation. Consequently, this is considered the initial stress response and can result in oxidative stress and damage to cell components [67]. This primarily occurs in chloroplasts, mitochondria, and peroxisomes in plants. To prevent excess ROS accumulation, the process of photorespiration is activated, dissipating excess reducing equivalents and energy through both direct and indirect mechanisms [68]. As part of these mechanisms, alternative metabolic pathways are engaged to restore cellular homeostasis. Malic acid, through the malate valve shuttle, plays a significant role in reducing excess equivalents in the chloroplasts [69, 70]. Moreover, under stress conditions, plants accumulate amino acids. The TCA cycle in plants becomes suppressed under stress, and the previously generated energy is redirected to accumulate amino acids, enhancing stress tolerance [71–73]. Shikimate, a core compound in the biosynthesis of aromatic amino acids like phenylalanine, tyrosine, and tryptophan, is particularly important [74]. Thus, metabolites related to the TCA cycle are crucial for interpreting the stress response and synthesizing secondary metabolites in plants, owing to their role in producing ATP and providing carbon skeletons for secondary metabolites [75]. In our current study, a significant increase in shikimate production was observed in basil plants that were grown under two conditions: T30 (T30/D11: 5.1 ± 6.9 μg/10 mg; T30/D23: 10.5 ± 0.8 μg/10 mg) and RA (T30/D11: 38.9 ± 6.9 mg/g; T30/D23: 35.1 ± 5.7 mg/g). Shikimate, which is the final product of the shikimate pathway, was also found highly quantified under the T30 condition. This observation is supported by a correlation coefficient (R-value) of 0.6906. These results suggest that photosynthesis under the T30 condition was functioning effectively and generating carbon skeletons that contributed to the production of the RA precursor. The superior photosynthetic efficiency under T30 conditions compared to other conditions can also be explained through identifiable growth patterns. Photosynthesis serves as a crucial determinant of plant biomass, yield, and metabolism. It enables the capture of solar energy, subsequently converting it into chemical molecules [76]. Carbohydrates produced through photosynthesis play dual roles, acting as signals and providing carbon for various plant metabolic processes and growth, including leaf development [77]. As shown in Table 4, carbohydrate (glucose) content was highly observed in T30 and T35 samples (27.7–99.0 μg/10 mg) but the T40 condition, which was extreme temperature stress, exhibited below 20 μg/10 mg content of glucose. Carbohydrate content provides insight into the potential impact of temperature variations on glucose production. Not only growth parameters linked to photosynthesis but also showed high in T30 conditions. In T30 conditions, both leaf length and leaf width, relative to lateral area, exhibited an expansion as light intensity decreased, and under consistent light conditions, with decreasing temperature. Furthermore, shoot length and internode length were markedly higher under T30 conditions, following a discernible trend of increase with decreasing temperature (Table 4).

The gradual reduction in leaf area and shoot length observed from T30 was considered to be a plant acclimatization strategy against temperature stress at T35 and T40. Various plant species have been documented to initiate acclimation responses during prolonged exposure to high temperatures, involving changes in morphological, physiological, and biochemical characteristics [78]. These morpho-physiological alterations, including diminished leaf area and photosynthesis, subsequently have a negative effect on vegetative stress and productivity [78]. In our study, the T35/D11 condition was identified as being under stress, as indicated by significantly elevated levels of various primary metabolites, including fumaric acid and malic acid. These changes can be attributed to the increased occurrence of photorespiration and the glyoxylate cycle, as documented in previous studies [69, 70]. It is important to note that secondary compounds, such as terpenes, can be synthesized to facilitate photorespiration, which serves as a protective mechanism for plants against oxidative stress and photodamage [79]. This observation aligns with our current findings.

As the stress intensity increased, particularly under the T40 extreme temperature stress condition, plants exhibited a notable accumulation of amino acids, which can act as a means of temperature stress resistance [80, 81]. Amino acids, being constituents of proteins, play diverse regulatory roles in abiotic stress responses. They can serve as signaling molecules, precursors for secondary metabolites, protein chaperones, and osmotic protectants [71]. Under temperature stress, plants accumulate specific amino acids, which can function as osmoprotectants to help maintain optimal balance, preserve redox homeostasis, and support metabolic processes [53, 71]. Aromatic amino acids, including phenylalanine, tyrosine, and tryptophan, are crucial precursors in protein synthesis and the synthesis of various natural products [82]. These amino acids are synthesized using the

Table 4 Primary metabolites of basil cultivated under different temperature and DLI

No	Compound Name	RI	T30		T35		T40	
			D11	D23	D11	D23	D11	D23
Organic acids								
1	Lactic Acid	1062	0.06 ± 0.01c	0.20 ± 0.02a	0.12 ± 0.03b	0.11 ± 0.01b	0.06 ± 0.00c	0.07 ± 0.01c
2	Glycolic acid	1077	0.07 ± 0.01b	0.05 ± 0.00 cd	0.04 ± 0.00d	0.04 ± 0.00d	0.06 ± 0.01bc	0.09 ± 0.01a
	Pyruvic acid	1091	0.05 ± 0.00b	0.10 ± 0.02a	0.05 ± 0.00b	0.10 ± 0.01a	0.10 ± 0.01a	0.09 ± 0.01a
6	Oxalic acid	1145	1.89 ± 0.15bc	2.57 ± 0.26a	1.77 ± 0.20c	2.29 ± 0.27ab	1.58 ± 0.16 cd	1.32 ± 0.22d
9	Malonic acid	1208	0.49 ± 0.03b	0.50 ± 0.03b	0.49 ± 0.05b	0.66 ± 0.10b	1.68 ± 0.19a	1.51 ± 0.20a
12	Maleic acid	1310	0.85 ± 0.10c	1.63 ± 0.11a	1.03 ± 0.12c	1.27 ± 0.08b	1.30 ± 0.16b	0.85 ± 0.06c
13	Succinic acid	1316	5.43 ± 1.00b	10.28 ± 0.77a	4.05 ± 0.41c	3.81 ± 0.22c	4.89 ± 0.95bc	6.01 ± 0.37b
14	Glyceric acid	1338	0.28 ± 0.04b	0.39 ± 0.04a	0.30 ± 0.03b	0.13 ± 0.02c	0.09 ± 0.01c	0.12 ± 0.01c
15	Fumaric acid	1348	0.80 ± 0.09c	1.06 ± 0.05b	1.40 ± 0.12a	0.60 ± 0.05d	0.55 ± 0.05d	0.65 ± 0.08d
17	Glutaric acid	1406	0.02 ± 0.01a	0.02 ± 0.00ab	0.02 ± 0.00ab	0.02 ± 0.00ab	0.02 ± 0.00b	0.02 ± 0.00ab
20	Malic acid	1498	54.18 ± 2.98b	60.97 ± 5.10ab	67.03 ± 5.88a	39.04 ± 4.39c	38.34 ± 2.80c	45.42 ± 3.38c
24	2-Oxoglutaric acid	1585	2.17 ± 0.39b	5.57 ± 0.90a	2.33 ± 0.35b	0.86 ± 0.14c	0.51 ± 0.07c	0.95 ± 0.17c
26	Tartaric acid	1653	31.87 ± 4.73b	43.40 ± 4.57a	38.16 ± 4.24ab	36.77 ± 3.17ab	39.55 ± 2.16a	38.81 ± 3.69ab
29	Putrescine	1747	0.11 ± 0.03b	0.26 ± 0.05a	0.12 ± 0.03b	0.21 ± 0.01a	0.08 ± 0.02b	0.08 ± 0.01b
32	Shikimic acid	1822	5.10 ± 0.86b	10.45 ± 0.76a	5.08 ± 0.43b	2.60 ± 0.29c	0.41 ± 0.07d	0.78 ± 0.05d
33	D-Glucuronic acid	1832	0.43 ± 0.08c	0.79 ± 0.12a	0.71 ± 0.07ab	0.65 ± 0.12ab	0.58 ± 0.04bc	0.76 ± 0.05a
34	Citric acid	1837	0.96 ± 0.15b	1.20 ± 0.15a	1.06 ± 0.13ab	0.95 ± 0.04b	1.00 ± 0.05ab	1.18 ± 0.04a
43	Ferulic acid	2104	0.03 ± 0.00bc	0.04 ± 0.00ab	0.02 ± 0.00c	0.05 ± 0.01a	0.05 ± 0.00a	0.05 ± 0.01a
44	Caffeic acid	2153	5.53 ± 0.45c	9.06 ± 0.73a	1.06 ± 0.13d	7.06 ± 0.74b	5.72 ± 0.49c	4.89 ± 0.25c
	Total		110.32 ± 6.96c	148.55 ± 9.31a	124.85 ± 10.42b	97.24 ± 3.86 cd	96.55 ± 2.07d	103.66 ± 3.94cd
Amino acids								
3	L-Valine	1090	0.93 ± 0.19d	1.99 ± 0.16c	0.97 ± 0.09d	2.96 ± 0.57b	4.86 ± 0.76a	4.11 ± 0.71a
5	L-Alanine	1106	0.02 ± 0.00b	0.01 ± 0.00b	0.03 ± 0.01b	0.03 ± 0.00b	0.29 ± 0.08a	0.24 ± 0.04a
7	L-Leucine	1159	0.85 ± 0.29c	1.41 ± 0.12b	0.58 ± 0.07c	1.55 ± 0.15ab	1.91 ± 0.20a	1.67 ± 0.27ab
8	L-Isoleucine	1181	0.82 ± 0.06d	1.37 ± 0.16c	0.65 ± 0.14d	1.89 ± 0.28b	2.50 ± 0.24a	2.02 ± 0.41b
10	L-Serine	1263	0.60 ± 0.06c	1.12 ± 0.05b	0.60 ± 0.08c	1.22 ± 0.16b	1.50 ± 0.12a	1.28 ± 0.12b
11	L-Threonine	1301	0.51 ± 0.07d	0.92 ± 0.07c	0.59 ± 0.10 cd	1.27 ± 0.14b	1.75 ± 0.21a	1.60 ± 0.30ab
16	L-Homoserine	1363	0.03 ± 0.00c	0.06 ± 0.02b	0.03 ± 0.00c	0.04 ± 0.01c	0.09 ± 0.02a	0.10 ± 0.01a
18	L-Aspartic acid	1429	0.51 ± 0.06c	0.94 ± 0.12b	0.49 ± 0.10c	0.61 ± 0.15c	1.78 ± 0.14a	0.90 ± 0.07b
19	β-Alanine	1435	ND	0.01 ± 0.00c	ND	ND	0.02 ± 0.00b	0.04 ± 0.01a
21	L-5-Oxoproline	1534	13.16 ± 0.81a	12.74 ± 0.69a	9.76 ± 1.22b	13.72 ± 1.72a	4.86 ± 0.46d	7.44 ± 0.50c
22	GABA	1537	0.01 ± 0.00d	0.04 ± 0.01c	ND	0.05 ± 0.01c	0.08 ± 0.02b	0.12 ± 0.01a
23	DL-Phenylalanine	1558	0.34 ± 0.07 cd	0.60 ± 0.05bc	0.29 ± 0.04d	0.84 ± 0.14b	2.04 ± 0.32a	0.39 ± 0.10 cd
25	L-Glutamic acid	1626	0.01 ± 0.00c	0.30 ± 0.01c	ND	0.16 ± 0.03c	2.15 ± 0.44b	2.77 ± 0.31a
31	L-Glutamine	1785	ND	ND	ND	ND	1.65 ± 0.09a	1.10 ± 0.11b
35	Asparagine	1886	0.48 ± 0.07c	0.85 ± 0.10c	0.46 ± 0.08c	2.07 ± 0.45a	1.42 ± 0.16b	1.88 ± 0.24a
40	L-Lysine	1936	0.04 ± 0.00d	0.10 ± 0.02bc	0.07 ± 0.00 cd	0.16 ± 0.03b	0.30 ± 0.03a	0.24 ± 0.06a
41	L-Tyrosine	1956	0.10 ± 0.01d	0.33 ± 0.05 cd	0.13 ± 0.03d	0.41 ± 0.05bc	1.19 ± 0.29a	0.66 ± 0.11b
	Total		18.40 ± 1.41c	22.79 ± 1.39b	14.66 ± 1.81c	26.97 ± 3.27a	28.38 ± 2.08a	26.56 ± 2.01ab
Carbohydrates								
27	D-Xylose	1675	0.29 ± 0.05b	0.48 ± 0.07a	0.31 ± 0.03b	0.16 ± 0.02c	0.15 ± 0.02c	0.15 ± 0.02c
28	D-Arabinose	1681	0.12 ± 0.02ab	0.16 ± 0.02a	0.13 ± 0.02ab	0.13 ± 0.04ab	0.10 ± 0.03b	0.11 ± 0.01ab
30	L-Rhamnose	1748	0.14 ± 0.02a	0.13 ± 0.01a	0.11 ± 0.01b	0.09 ± 0.00bc	0.08 ± 0.01c	0.08 ± 0.01c
36	Fructose	1902	5.93 ± 1.23a	6.77 ± 0.66a	6.32 ± 0.89a	2.88 ± 0.73b	2.52 ± 0.26b	2.02 ± 0.22b
37	Mannose	1917	0.06 ± 0.01a	0.06 ± 0.01a	0.05 ± 0.01a	0.03 ± 0.01b	0.02 ± 0.00b	0.03 ± 0.01b
38	Galactose	1923	6.54 ± 1.07ab	7.43 ± 1.32a	5.31 ± 0.69bc	3.98 ± 0.59cd	4.27 ± 0.55cd	3.39 ± 0.38d
39	Glucose	1929	43.48 ± 7.95c	98.97 ± 6.86a	53.97 ± 4.69b	27.65 ± 3.32d	12.24 ± 1.75e	16.04 ± 3.13e

Table 4 (continued)

No	Compound Name	RI	T30		T35		T40	
			D11	D23	D11	D23	D11	D23
49	Sucrose	2590	3.97 ± 0.84 cd	6.54 ± 0.44a	3.97 ± 0.51 cd	5.30 ± 0.31b	3.62 ± 0.25d	4.90 ± 0.35bc
	Total		60.52 ± 9.93b	120.56 ± 7.99a	70.16 ± 6.22b	40.21 ± 2.92c	23.00 ± 2.32d	26.71 ± 3.76d
Fatty acids								
42	Palmitic Acid	2050	2.87 ± 0.51bc	2.90 ± 0.17bc	4.52 ± 0.67a	3.42 ± 0.19b	2.75 ± 0.24bc	2.31 ± 0.20c
45	Linoleic acid	2215	0.21 ± 0.03ab	0.30 ± 0.05a	0.18 ± 0.06b	0.23 ± 0.03ab	0.22 ± 0.03ab	0.24 ± 0.06ab
46	Oleic Acid	2220	0.01 ± 0.00b	0.01 ± 0.00b	0.01 ± 0.00a	0.01 ± 0.00b	0.01 ± 0.00b	0.01 ± 0.00ab
47	α-Linolenic acid	2223	0.30 ± 0.02b	0.36 ± 0.02a	0.33 ± 0.03ab	0.37 ± 0.03a	0.37 ± 0.04a	0.37 ± 0.01a
48	Stearic acid	2245	1.02 ± 0.12ab	1.14 ± 0.06a	1.26 ± 0.23a	1.27 ± 0.16a	0.87 ± 0.05b	0.81 ± 0.07b
	Total		4.41 ± 0.60bcd	4.71 ± 0.25bc	6.30 ± 0.86a	5.29 ± 0.38b	4.22 ± 0.24cd	3.74 ± 0.31d

Each group used five individuals as biological replicates and values are the means ± standard deviation (μg/10 mg). Same lower cases represent non-significant difference and different lower cases (a–d) in the same row represent statistically significant differences among the groups according to Tukey HSD Test ($p < 0.05$). RI, retetion index; ND, not detected

carbon skeleton provided by the shikimate pathway [83, 84]. Consequently, phenylalanine and tyrosine, as products of the shikimate pathway and intermediates in the RA (rosmarinic acid) and VOCs biosynthesis pathway, were found highly quantified in both the T40 condition (both in D11 and D23). This resulted in a negative correlation between amino acids and RAC (phenylalanine, r = − 0.4073; tyrosine, r = − 0.6695) and shikimate (phenylalanine, r = − 0.4249; tyrosine, r = − 0.5928). Furthermore, glutamine and glutamic acid, which contribute to balance homeostasis in plants by exporting into the cytoplasm and converting to GABA (gamma-aminobutyric acid) [85], also exhibited a significant increase under the T40 condition.

In plants, continuous stress treatments lasting for days or weeks lead to an acclimation process [86]. In this study, both the maintenance/enhancement of growth and the enhancement of functional components were achieved by inducing adaptive mechanisms in basil through long-term treatments. The responses to temperature and light intensity were interpreted based on metabolic changes.

Conclusion

In plants, continuous stress treatments lasting for days or weeks lead to an acclimation process that enhances stress tolerance, resulting in higher survival rates and increased production. Therefore, long-term cultivation conditions with different temperatures (T30, T35, and T40) and DLI (D11 and D23) were applied to basil cultivation and morphological and biochemical (primary and secondary metabolites) investigations in plants were performed to obtain a comprehensive understanding. As growth progressed, the growth parameters gradually displayed differences, indicating that treatment conditions induced morphological changes in basil plants, and it was interpreted as associated with metabolites. The larger leaf area, longer shoot length, and internode length of T30 were attributed to effective photosynthesis, resulting in a higher amount of carbohydrates and these served as generating carbon skeletons for the TCA cycle. Consequently, higher organic acids, in particular shikimate, are attributed to RA precursor. Meanwhile, along with the temperature increase, reduced leaf area was observed and as the assimilation process, plants stimulated a balance in homeostasis against the accumulated reactive oxygen species (ROS). As a part of this response, plants stimulate transpiration, consequently, fumaric acid and malic acid, which are involved in the glyoxylate pathway, and emission of VOCs were increased under T35/T11. Furthermore, under the more intense heat stress conditions of T40, an extreme accumulation of amino acids was observed, suggesting an adaptation mechanism for survival.

Abbreviations

ANOVA	Analysis of variance
DLI	Daily light integral
GC-TOF–MS	Gas chromatogram-time of flight-mass
HPLC	High performance liquid chromatogram
HS	Head space
PPFD	Photosynthetic photon flux density
RA	Rosmarinic acid
RAC	Rosmarinic acid content
ROS	Reactive oxygen species
SPME	Solid-phase microextraction
TCA	Tricarboxylic acid
TPC	Total phenolics content
VOCs	Volatile organic compounds

Supplementary Information

The online version contains supplementary material available at https://doi.org/10.1186/s40538-023-00532-2.

Additional file 1: Fig. S1. Typical HPLC chromatogram of basil (2 mg/mL) detected at 330 nm. RA was observed at 11.94 min as the major compound and the calibration curves were constructed by plotting the peak area of RA against diverse concentrations ranging from 5 µg/ml to 200 µg/mL.

Additional file 2: Fig. S2. HS-SPME-GC-ToF–MS total ion chromatogram (TIC) of basil sample. Main compounds of volatiles were composed with linalool and eugenol.

Acknowledgements
This research was funded by an Intramural Grant (2Z06831) from the Korea Institute of Science and Technology (KIST); This research was supported by the National Research Council of Science & Technology (NST) grant by the Korea government (MSIT) (No. CPS22041-110).

Authors contributions
DHR: Conceptualization, Investigation, Writing-original draft. JYC: Investigation. Methodology, Writing-review & editing. MH: Writing-review & editing. DGL: Investigation. HYK: Project administration, Supervision, Writing-review & editing.

Funding
Korea Institute of Science and Technology, South Korea, 2Z06831

Availability of data and materials
The datasets used and/or analysed during the current study are available from the corresponding author on reasonable request.

Declarations

Ethics approval and consent to participate
The study did not use any animal or human subjects; hence, ethical approval or volunteer consent was not required.

Consent for publication
The authors give consent for the publication and its relevant data.

Competing interests
No conflict of interest exists among the authors.

Author details
[1]Smart Farm Research Center, Korea Institute of Science and Technology (KIST), Gangneung, Gangwon 25451, Republic of Korea. [2]Division of Bio-Medical Science and Technology, KIST School, Korea University of Science and Technology (UST), Daejeon 34113, Republic of Korea. [3]Department of Botany, Garden Campus, Abdul Wali Khan University Mardan, Nowshera Mardan Rd, Mardan 23200, Pakistan.

Received: 12 November 2023 Accepted: 28 December 2023
Published online: 15 January 2024

References

1. Jin H, Zhu Z. Dark, light, and temperature: key players in plant morphogenesis. Plant Physiol. 2019;180(4):1793–802.
2. Franklin KA. Light and temperature signal crosstalk in plant development. Curr Opin Plant Biol. 2009;12(1):63–8.
3. Janda T, Prerostová S, Vanková R, Darkó É. Crosstalk between light-and temperature-mediated processes under cold and heat stress conditions in plants. Int J Mol Sci. 2021;22(16):8602.
4. Cheng M-C, Kathare PK, Paik I, Huq E. Phytochrome signaling networks. Annual Rev Plant Biol. 2021;72(1):217–44.
5. Ding Y, Shi Y, Yang S. Molecular regulation of plant responses to environmental temperatures. Mol Plant. 2020;13(4):544–64.
6. Quint M, Delker C, Franklin KA, Wigge PA, Halliday KJ, Van Zanten M. Molecular and genetic control of plant thermomorphogenesis. Nature plants. 2016;2(1):1–9.
7. Sun J, Qi L, Li Y, Chu J, Li C. PIF4–mediated activation of YUCCA8 expression integrates temperature into the auxin pathway in regulating Arabidopsis hypocotyl growth. PLoS Genet. 2012;8(3): e1002594.
8. Xu Y, Zhu Z. PIF4 and PIF4-interacting proteins: at the nexus of plant light, temperature and hormone signal integrations. Int J Mol Sci. 2021;22(19):10304.
9. Koini MA, Alvey L, Allen T, Tilley CA, Harberd NP, Whitelam GC, et al. High temperature-mediated adaptations in plant architecture require the bHLH transcription factor PIF4. Curr Biol. 2009;19(5):408–13.
10. Ma D, Li X, Guo Y, Chu J, Fang S, Yan C, et al. Cryptochrome 1 interacts with PIF4 to regulate high temperature-mediated hypocotyl elongation in response to blue light. Proc Natl Acad Sci. 2016;113(1):224–9.
11. Guo H, Yang H, Mockler TC, Lin C. Regulation of flowering time by Arabidopsis photoreceptors. Science. 1998;279(5355):1360–3.
12. Karayekov E, Sellaro R, Legris M, Yanovsky MJ, Casal JJ. Heat shock–induced fluctuations in clock and light signaling enhance phytochrome B–mediated arabidopsis deetiolation. Plant Cell. 2013;25(8):2892–906.
13. Legris M, Nieto C, Sellaro R, Prat S, Casal JJ. Perception and signalling of light and temperature cues in plants. Plant J. 2017;90(4):683–97.
14. Qin L, Li C, Li D, Wang J, Yang L, Qu A, et al. Physiological, Metabolic and transcriptional responses of Basil (*Ocimum basilicum* Linn. var. pilosum (Willd.) Benth.) to Heat Stress. Agronomy. 2022;12(6):1434.
15. Akula R, Ravishankar GA. Influence of abiotic stress signals on secondary metabolites in plants. Plant Signal Behav. 2011;6(11):1720–31.
16. Geng X-M, Liu X, Ji M, Hoffmann WA, Grunden A, Xiang Q-YJ. Enhancing heat tolerance of the little dogwood *Cornus canadensis* L. f. with introduction of a superoxide reductase gene from the hyperthermophilic archaeon *Pyrococcus furiosus*. Front Plant Sci. 2016;7:26.
17. Irato P, Santovito G. Enzymatic and non-enzymatic molecules with antioxidant function. MDPI. 2021;10:579.
18. Erb M, Kliebenstein DJ. Plant secondary metabolites as defenses, regulators, and primary metabolites: the blurred functional trichotomy. Plant Physiol. 2020;184(1):39–52.
19. Anulika NP, Ignatius EO, Raymond ES, Osasere O-I, Abiola AH. The chemistry of natural product: plant secondary metabolites. Int J Technol Enhancem Emerg Eng Res. 2016;4(8):1–9.
20. Nadeem M, Imran M, Aslam Gondal T, Imran A, Shahbaz M, Muhammad Amir R, et al. Therapeutic potential of rosmarinic acid: a comprehensive review. Appl Sci. 2019;9(15):3139.
21. Salar E, Khavari-Nejad R, Mandoulakani BA, Najafi F. Effects of TiO2 Nanoparticles on Activity of Antioxidant Enzymes, the Expression of Genes Involved in Rosmarinic Acid Biosynthesis and Rosmarinic Acid Content in *Dracocephalum kotschyi* Boiss. Russ J Plant Physiol. 2021;68(1):118–25.
22. Pirooz P, Amooaghaie R, Ahadi A, Sharififar F, Torkzadeh-Mahani M. Silicon and nitric oxide synergistically modulate the production of essential oil and rosmarinic acid in *Salvia officinalis* under Cu stress. Protoplasma. 2022;259(4):905–16.
23. Benedec D, Hanganu D, Oniga I, Tiperciuc B, Olah N-K, Raita O, et al. Assessment of rosmarinic acid content in six Lamiaceae species extracts and their antioxidant and antimicrobial potential. Pak J Pharm Sci. 2015;28(6):2297–303.
24. Bahcesular B, Yildirim ED, Karaçocuk M, Kulak M, Karaman S. Seed priming with melatonin effects on growth, essential oil compounds and antioxidant activity of basil (*Ocimum basilicum* L.) under salinity stress. Ind Crops Prod. 2020;146: 112165.
25. Sakkas H, Papadopoulou C. Antimicrobial activity of basil, oregano, and thyme essential oils. J Microbiol Biotechnol. 2017;27(3):429–38.
26. Juliani H, Simon J. Antioxidant activity of basil. Trends New Crops New Uses. 2002;575(9):575–9.
27. Oxenham S, Svoboda K, Walters D. Antifungal activity of the essential oil of basil (*Ocimum basilicum*). J Phytopathol. 2005;153(3):174–80.
28. Blande JD, Glinwood R. Deciphering chemical language of plant communication: Springer; 2016.

29. Widhalm JR, Jaini R, Morgan JA, Dudareva N. Rethinking how volatiles are released from plant cells. Trends Plant Sci. 2015;20(9):545–50.
30. Baldwin IT. Plant volatiles. Curr Biol. 2010;20(9):R392–7.
31. Lu N, Bernardo EL, Tippayadarapanich C, Takagaki M, Kagawa N, Yamori W. Growth and accumulation of secondary metabolites in perilla as affected by photosynthetic photon flux density and electrical conductivity of the nutrient solution. Front Plant Sci. 2017;8:708.
32. Shabani L, Razavizadeh R. Chitosan enhances rosmarinic acid production in shoot cultures of *Melissa officinalis* L. through the induction of methyl jasmonate. Bot Stud. 2019;60(1):1–10.
33. Walters KJ, Currey CJ. Growth and development of basil species in response to temperature. HortScience. 2019;54(11):1915–20.
34. Shen Y, Jin L, Xiao P, Lu Y, Bao J. Total phenolics, flavonoids, antioxidant capacity in rice grain and their relations to grain color, size and weight. J Cereal Sci. 2009;49(1):106–11.
35. Park MJ, Cho JY, Ha IJ, Moon JS, Kang Y-H. Comparison of the antioxidant properties and flavonols in various parts of Korean red onions by multivariate data analysis. Horticult Environ Biotechnol. 2018;59(6):919–27.
36. Re R, Pellegrini N, Proteggente A, Pannala A, Yang M, Rice-Evans C. Antioxidant activity applying an improved ABTS radical cation decolorization assay. Free Radical Bio Med. 1999;26(9–10):1231–7.
37. Xu JL, Kim TJ, Kim J-K, Choi Y. Simultaneous roasting and extraction of green coffee beans by pressurized liquid extraction. Food Chem. 2019;281:261–8.
38. Jorge TF, Duro N, Da Costa M, Florian A, Ramalho JC, Ribeiro-Barros AI, et al. GC-TOF-MS analysis reveals salt stress-responsive primary metabolites in *Casuarina glauca* tissues. Metabolomics. 2017;13:1–13.
39. Copolovici L, Copolovici DM, Moisa C, Lupitu A. Antagonist temperature variation affects the photosynthetic parameters and secondary metabolites of *Ocimum basilicum* L. and *Salvia officinalis* L. Plants. 2022;11(14):1806.
40. Bita CE, Gerats T. Plant tolerance to high temperature in a changing environment: scientific fundamentals and production of heat stress-tolerant crops. Front Plant Sci. 2013;4:273.
41. Mosadegh H, Trivellini A, Ferrante A, Lucchesini M, Vernieri P, Mensuali A. Applications of UV-B lighting to enhance phenolic accumulation of sweet basil. Sci Hortic. 2018;229:107–16.
42. Kwee EM, Niemeyer ED. Variations in phenolic composition and antioxidant properties among 15 basil (*Ocimum basilicum* L.) cultivars. Food Chem. 2011;128(4):1044–50.
43. Złotek U, Szymanowska U, Karaś M, Świeca M. Antioxidative and anti-inflammatory potential of phenolics from purple basil (*Ocimum basilicum* L.) leaves induced by jasmonic, arachidonic and β-aminobutyric acid elicitation. Int J Food Sci Technol. 2016;51(1):163–70.
44. Shiga T, Shoji K, Shimada H, Hashida S, Goto F, Yoshihara T. Effect of light quality on rosmarinic acid content and antioxidant activity of sweet basil, Ocimum basilicum L. Plant Biotechnol. 2009;26(2):255–9.
45. Shekarchi M, Hajimehdipoor H, Saeidnia S, Gohari AR, Hamedani MP. Comparative study of rosmarinic acid content in some plants of Labiatae family. Pharmacogn Mag. 2012;8(29):37.
46. Meng L, Lozano YF, Gaydou EM, Li B. Antioxidant activities of polyphenols extracted from *Perilla frutescens* varieties. Molecules. 2009;14(1):133–40.
47. Canadanovic-Brunet J, Cetkovic G, Djilas S, Tumbas V, Bogdanović G, Mandic A, et al. Radical scavenging, antibacterial, and antiproliferative activities of *Melissa officinalis* L. extracts. J Med Food. 2008;11(1):133–43.
48. Trivellini A, Lucchesini M, Maggini R, Mosadegh H, Villamarin TSS, Vernieri P, et al. Lamiaceae phenols as multifaceted compounds: bioactivity, industrial prospects and role of "positive-stress." Ind Crops Prod. 2016;83:241–54.
49. Lee C-J, Chen L-G, Chang T-L, Ke W-M, Lo Y-F, Wang C-C. The correlation between skin-care effects and phytochemical contents in Lamiaceae plants. Food Chem. 2011;124(3):833–41.
50. Zare M, Ganjeali A, Lahouti M. Rosmarinic and caffeic acids contents in Basil (*Ocimum basilicum* L.) are altered by different levels of phosphorus and mycorrhiza inoculation under drought stress. Acta Physiol Plant. 2021;43:1–10.
51. Moazzami Farida SH, Karamian R, Albrectsen BR. Silver nanoparticle pollutants activate oxidative stress responses and rosmarinic acid accumulation in sage. Physiol Plant. 2020;170(3):415–32.
52. Fletcher RS, Slimmon T, McAuley CY, Kott LS. Heat stress reduces the accumulation of rosmarinic acid and the total antioxidant capacity in spearmint (*Mentha spicata* L). J Sci Food Agric. 2005;85(14):2429–36.
53. Sahu R, Gangopadhyay M, Dewanjee S. Elicitor-induced rosmarinic acid accumulation and secondary metabolism enzyme activities in Solenostemon scutellarioides. Acta Physiol Plant. 2013;35:1473–81.
54. Jakovljević D, Momčilović J, Bojović B, Stanković M. The short-term metabolic modulation of basil (*Ocimum basilicum* L. cv.'Genovese') after exposure to cold or heat. Plants. 2021;10(3):590.
55. Castronuovo D, Russo D, Libonati R, Faraone I, Candido V, Picuno P, et al. Influence of shading treatment on yield, morphological traits and phenolic profile of sweet basil (*Ocimum basilicum* L.). Sci Horticultur. 2019;254:91–8.
56. Pennisi G, Pistillo A, Orsini F, Cellini A, Spinelli F, Nicola S, et al. Optimal light intensity for sustainable water and energy use in indoor cultivation of lettuce and basil under red and blue LEDs. Sci Hortic. 2020;272:109508.
57. Zhou R, Yu X, Li X, Mendanha dos Santos T, Rosenqvist E, Ottosen C-O. Combined high light and heat stress induced complex response in tomato with better leaf cooling after heat priming. Plant Physiol Biochem. 2020;151:1–9.
58. Tiwari S, Kate A, Mohapatra D, Tripathi MK, Ray H, Akuli A, et al. Volatile organic compounds (VOCs): Biomarkers for quality management of horticultural commodities during storage through e-sensing. Trends Food Sci Technol. 2020;106:417–33.
59. Niederbacher B, Winkler J, Schnitzler J. Volatile organic compounds as non-invasive markers for plant phenotyping. J Exp Bot. 2015;66(18):5403–16.
60. Abdollahi Mandoulakani B, Eyvazpour E, Ghadimzadeh M. The effect of drought stress on the expression of key genes involved in the biosynthesis of phenylpropanoids and essential oil components in basil (*Ocimum basilicum* L.). Phytochemistry. 2017;139:1–7.
61. Rezaie R, Abdollahi Mandoulakani B, Fattahi M. Cold stress changes antioxidant defense system, phenylpropanoid contents and expression of genes involved in their biosynthesis in *Ocimum basilicum* L. Sci Rep. 2020;10(1):5290.
62. Walters KJ, Lopez RG. Hydroponic Basil production: temperature influences volatile organic compound profile, but not overall consumer preference. Horticulturae. 2022;8(1):76.
63. Zaynab M, Fatima M, Sharif Y, Zafar MH, Ali H, Khan KA. Role of primary metabolites in plant defense against pathogens. Microb Pathog. 2019;137: 103728.
64. Barnabás B, Jäger K, Fehér A. The effect of drought and heat stress on reproductive processes in cereals. Plant Cell Environ. 2008;31(1):11–38.
65. Hasanuzzaman M, Nahar K, Alam MM, Roychowdhury R, Fujita M. Physiological, biochemical, and molecular mechanisms of heat stress tolerance in plants. Int J Mol Sci. 2013;14(5):9643–84.
66. Król A, Amarowicz R, Weidner S. Changes in the composition of phenolic compounds and antioxidant properties of grapevine roots and leaves (*Vitis vinifera* L.) under continuous of long-term drought stress. Acta Physiol Plant. 2014;36:1491–9.
67. Paul MJ, Pellny TK. Carbon metabolite feedback regulation of leaf photosynthesis and development. J Exp Bot. 2003;54(382):539–47.
68. Apel K, Hirt H. Reactive oxygen species: metabolism, oxidative stress, and signal transduction. Annu Rev Plant Biol. 2004;55:373–99.
69. Voss I, Sunil B, Scheibe R, Raghavendra A. Emerging concept for the role of photorespiration as an important part of abiotic stress response. Plant Biol. 2013;15(4):713–22.
70. Dao O, Kuhnert F, Weber APM, Peltier G, Li-Beisson Y. Physiological functions of malate shuttles in plants and algae. Trends Plant Sci. 2022;27(5):488–501.
71. Crecelius F, Streb P, Feierabend J. Malate metabolism and reactions of oxidoreduction in cold-hardened winter rye (*Secale cereale* L.) leaves. J Exper Botany. 2003;54(384):1075–83.
72. Wang J, Yuan B, Xu Y, Huang B. Differential responses of amino acids and soluble proteins to heat stress associated with genetic variations in heat tolerance for hard fescue. J Am Soc Hortic Sci. 2018;143(1):45–55.
73. You J, Zhang Y, Liu A, Li D, Wang X, Dossa K, et al. Transcriptomic and metabolomic profiling of drought-tolerant and susceptible sesame genotypes in response to drought stress. BMC Plant Biol. 2019;19(1):1–16.

74. Trovato M, Funck D, Forlani G, Okumoto S, Amir R. Amino acids in plants: regulation and functions in development and stress defense. Front Media SA. 2021;12:772810.
75. Zabalza A, Orcaray L, Fernández-Escalada M, Zulet-González A, Royuela M. The pattern of shikimate pathway and phenylpropanoids after inhibition by glyphosate or quinate feeding in pea roots. Pestic Biochem Physiol. 2017;141:96–102.
76. Daloso DM, Müller K, Obata T, Florian A, Tohge T, Bottcher A, et al. Thioredoxin, a master regulator of the tricarboxylic acid cycle in plant mitochondria. Proc Natl Acad Sci. 2015;112(11):E1392–400.
77. Muhie SH. Optimization of photosynthesis for sustainable crop production. CABI Agric Biosci. 2022;3(1):1–8.
78. Vasseur F, Pantin F, Vile D. Changes in light intensity reveal a major role for carbon balance in Arabidopsis responses to high temperature. Plant Cell Environ. 2011;34(9):1563–76.
79. Kaur N, Snider JL, Parkash V, Paterson AH, Grey TL, Tishchenko V. Genotypic variation in growth, single leaf physiology, and acclimation potential of thylakoid processes in cotton exposed to high temperature extremes. Environ Exp Bot. 2023;215: 105512.
80. Kopaczyk JM, Warguła J, Jelonek T. The variability of terpenes in conifers under developmental and environmental stimuli. Environ Exp Bot. 2020;180: 104197.
81. Kosová K, Vítámvás P, Prášil IT, Renaut J. Plant proteome changes under abiotic stress—contribution of proteomics studies to understanding plant stress response. J Proteomics. 2011;74(8):1301–22.
82. Zhang L, Garneau MG, Majumdar R, Grant J, Tegeder M. Improvement of pea biomass and seed productivity by simultaneous increase of phloem and embryo loading with amino acids. Plant J. 2015;81(1):134–46.
83. Kisa D, İmamoğlu R, Genç N, Şahin S, Qayyum MA, Elmastaş M. The interactive effect of aromatic amino acid composition on the accumulation of phenolic compounds and the expression of biosynthesis-related genes in *Ocimum basilicum*. Physiol Mol Biol Plants. 2021;27(9):2057–69.
84. Tohge T, Watanabe M, Hoefgen R, Fernie AR. Shikimate and phenylalanine biosynthesis in the green lineage. Front Plant Sci. 2013;4:62.
85. Weaver LM, Herrmann KM. Dynamics of the shikimate pathway in plants. Trends Plant Sci. 1997;2(9):346–51.
86. Qiu X-M, Sun Y-Y, Ye X-Y, Li Z-G. Signaling role of glutamate in plants. Front Plant Sci. 2020;10:1743.

Publisher's Note